



Université Mohamed Khider de
Biskra Faculté Des Sciences Et
De La Technologie
Département de génie
mécanique

MÉMOIRE DE MASTER

Domaine : Sciences et Techniques

Filière : Génie Mécanique

Spécialité : Energétique

Réf. : Entrez la référence du document

Présenté et soutenu par :

THELIB ATMANE

Le : [Click here to enter a date.](#)

Numerical study of heat transfer associated with mass transfer inside a cavity

Jury :

Mr	Chawki MAHBOUB	MCB	Université de Biskra	Président
Mr	SALAH GUERBAAI	MCA	Université de Biskra	Rapporteur
Ms	Noura BOULTIF	MCB	Université de Biskra	Examineur

Année universitaire : 2021 - 2022

DEDICACE

First of all I want to thank ALLAH for giving me this opportunity to live and study at this amazing university and providing all what I need to gain a lot knowledge and share a nice memories with nice people. I hope that ALLAH guides us for our next step in our life.

Second, I want to thank my mother for all her unconditionally love and patient for rising me and help me from the second I born till now, And I want to say that I love her so much and I admire her a lot and she is the only person who deserve to be on this thanking paper.

Finally, I want to thank myself for doing all the hard work and never give up, I want to thank myself for being patient and dedicated for my dreams and goals.

Acknowledgements

I would like to express my sincere thanks to my advisor, Dr. Salah GUERBAAI for his support and suggestions. this thesis cannot be done correctly in this short period without his guidance.

I would like to express my sincere gratitude to the committee members, Dr. Noura BOULTIF and Dr. Chawki MAHBOUB.

A special thanks for my professors Pr. Abd moumen hakim BENMACHICHE and Pr. Nour eddine BELGHAR for their continuous motivation and encouragement.

I would like to thank all the teachers of the department of mechanical engineering specially: Dr. Belhi GUERIRA, Dr. Miloud ZELLOUF, Dr. mohamed said CHEBAH...

Thanks for all friends and families.

Abstract

The aim of this study was to investigate steady state double diffusive mixed convection in a rectangular lid driven cavity while the bottom wall heated uniformly and the side walls are linearly heated which are hot at the bottom and cooled at the top. The top of the cavity (Top wall) is adiabatic and for the mass, a high and regularly concentrated wall at the left and a lower concentration but regularly too at the right wall while the horizontal walls are maintained impermeable. The governing equations are presented in dimensional form and non dimensional form then discretized using finite volume method after that solving this discretized system using SIMPLE algorithm to get the different gradients like velocities, temperature and concentration and the iterative method used for solving the system of equations is TDMA and all this processes programmed with Fortran software. The heat and mass transfer rates were examined using several operational dimensionless parameters such as Richardson number Ri , Lewis number Le , Buoyancy ratio N , Aspect ratio A . while $Pr=10$ and $Re=100$. also a Nusselt and Sherwood number for the local and the average are extracted and plotted by Origin 2022. The isocontours of the different physical quantities like streamlines, isocontours and isotherms are depicted with software Tecplot 360.

Keywords: Mixed convection, Lid driven cavity, Finite volume method, Heat and mass transfer, Numerical simulation

ملخص:

الهدف من هذه العمل هو القيام بدراسة عددية لانتقال الكتلة و الحرارة لتدفق داخل تجويف ذو شكل رباعي قائم, هذا التجويف تحت تأثير الحمل الحراري المزوج. حيث تم تسخين قاع التجويف بحرارة ثابتة على مستوى هذا السطح, بينما تم تسخين الجدارين الجانبين بحرارة متغيرة خطيا حيث أسفل الجدار ساخن و أعلاه بارد اما الجدار العلوي يكون معزولا حراريا و يتحرك بسرعة افقية ثابتة, بينما تركيز الكتلة منتظم و كبير في الجدار الأيسر و اقل تركيزا في الجدار الأيمن. تمت نمذجة المعدلات التي يخضع لها هذا النموذج المدروس و كذا الشروط الحدية و الابتدائية. تم تعريف المجال باستعمال طريقة الحجم المحدودة و اعتماد خوارزمية SIMPLE لاقتزان السرعة مع الضغط, لحساب مختلف القيم الفيزيائية مثل السرعة, الحرارة و التركيز. تحل المعادلات الجبرية باستعمال TDMA. تم التغيير في Ri و A , Le , N لرؤية تأثيرهم على التدفق. النتائج المتحصل عليها تم عرضها عن طريق دالة تيار, انتشار الحرارة و انتشار التركيز داخل التجويف و كذا قيم الموضعية و المتوسطة لعدد نوسالت Nu و عدد شاروود Sh باستعمال برنامج Techplot 360 و Origin 2022.

الكلمات المفتاحية : الحمل الحراري المزوجة, تجويف مدفوع, طريقة الحجم المحدودة, انتقال الحراري و الكتلي, دراسة عددية.

Résumé:

L'objectif de ce travail est de faire une étude numérique du transfert de masse et de chaleur pour un écoulement dans une cavité rectangulaire, cette cavité est sous l'effet d'une double convection où le fond de cette cavité était chauffé par une température uniforme, tandis que les murs des deux côtés étaient chauffés de la même manière d'une façon linéaire où le bas de ces murs est chaud et l'haute est maintenue froide, la paroi supérieure est adiabatique, La paroi gauche est plus concentrée que la paroi droite et les parois horizontales sont imperméables. Les équations qui gouvernent le modèle physique est représenté sous forme dimensionnelle et adimensionnelle ainsi que les conditions aux limites et initiales est aussi. Le Domain étudiée a été défini et discrétisée à l'aide de la méthode des volumes finis et de l'algorithme SIMPLE de couplage de la vitesse à la pression, Une méthode pour résoudre l'ensemble d'équations pour obtenir les grandeurs physiques est TDMA. Les nombres adimensionnels A , Le , N et Ri sont variés pour voir leur effet à l'écoulement. Les résultats obtenus ont été présentés en fonction du courant, de contour de température et de contour de la concentration, ainsi que des valeurs locales et moyennes du nombre Nu et du nombre Sh en utilisant Tecplot 360 et Origin 2022.

Mots clés : convection mixte, cavité entraînée, méthode des volumes finis, transfert de masse et thermique, étude numérique.

I-2-2-3-Mass transfer by change of phase.....	8
I-2-3-Fick's Law.....	8
I-2-4-General equation of mass transfer.....	9
I-2-5-Dimensionless Numbers.....	9
1-Sherwood Number.....	9
2-Schmidt Number.....	9
3-Lewis Number.....	9
4-Buoyancy ratio.....	10
I-3-Reviews.....	10
I-4-Conclusion.....	11
Chapter II:Problem description and mathematical formulation.....	12
II-1-Introduction.....	12
II-2-Problem description.....	12
II-3-Hypotheses.....	13
II-4-Mathelatical formulation.....	13
II-4-1-Mass conservation.....	13
II-4-2-Momentum equation.....	13
II-4-3-Energie equation	13
II-4-4-Concentration equation	13
II-5-Boundary conditions	14
II-6-Dimensionless groups	14
II-7-Dimensionless governing equations.....	14
II-8-Dimensionless boundary conditions.....	15
II-9-Nusselt number.....	15
II-10-Sherwood number	15
II-11-The stream function.....	16
II-12-Conclusion.....	16
Chapter III: Resolution method.....	17
III-1-Introduction	17
III-2-Transport equation	18
III-3-Staggered grid.....	18
III-4-The central differential scheme	19
III-5-Discretisation of transport equation	19
III-6-The discretisation schemes.....	22
III-7-Implementation of boundary conditions.....	23
III-8-Solution of discretized equation.....	24
III-8-1-TDMA Algorithm.....	24
III-9-SIMPLE Algorithm.....	25
III-10-Conclusion.....	30
Chapter IV: Results and discussion.....	31
IV-1-Introduction.....	31
IV-2-Algorithm validation.....	31
IV-2-1-The Local Nusselt number.....	32

IV-2-2-The average Nusselt number	33
IV-3-Comparative study with previous works.....	34
1-First validation.....	34
2-Second validation.....	36
3-An additional confirmation.....	39
IV-4-Results and discussion.....	39
IV-4-1-First case: effect of Lewis number Le	40
IV-4-2-Second case: effect of buoyancy ratio N	44
IV-4-3-Third case: effect of Richardson number Ri	49
IV-4-4-Fourth case: effect of Aspect ratio A	53
IV-5-Conclusion.....	57
GENERAL CONCLUSION.....	58
REFERENCES.....	59

Figures list:

Figure II.1 a schematic physical model.....	12
Figure III.1 : Staggered grid scheme	18
Figure III.2 : central differential scheme.....	19
Figure III.3 : SIMPLE Algorithm	29
Figure IV.1:used mesh.....	31
Figures IV.2 : variation of Nusselt Numbers along the walls for different mesh grids.....	32
Figure IV.3 : average Nusselt number at different walls for different grid mesh.....	33
Figure IV.4: isocontours of the present study and [9] for $Le=0.1$ $Le=1$	34
Figure IV.5: isocontours of the present study and [9] for $Le=25$ and $Le=50$	35
Figure IV.6: isocontours of the present study and [10] for $Le=1$	36
Figure IV.7: isocontours of the present study and [10] for $Le=10$	37
Figure IV.8: isocontours of the present study and [10] for $Le=50$	38
Figure IV.9: average Nusselt number varying with N for present code and [9],[10]codes for the work of [9].....	39
Figure IV.10: the effect of Lewis number on the isocontours for $N=1$, $Ri=1$, $A=1$, $Pr=10$	41
Figures IV.11: Nusselt number for Different walls $A=1$, $N=1$, $Ri=1$	42
Figure IV.12: the average Nusselt number at the different walls varied with Le	43
Figure IV.13:Local and average Sherwood number at the left wall varied with Le , $N=1$, $Ri=1$, $A=1$	43

Figure IV.14: Effect of buoyancy ratio on the isocontours for $Le=1$, $Ri=1, A=1, Pr=10$	46
Figure IV.15 : Nusselt number at the different walls varying with N while $Le=1, Ri=1, A=1$	47
Figure IV.16 : The average Nusselt number at the different wall varied with N	48
Figure IV.17 : Local and average Sherwood number varied with N , While $Le=1, Ri=1, A=1$ at the left wall.....	48
Figure IV.18:the effect of the Ri number on the isocontours while $Le=1, N=1, A=1, Pr=10$	50
Figure IV.19: Nusselt number at the different walls for $Le=1, N=1, A=1$	51
Figure IV.20: the average Nusselt number varied with Ri for different walls.....	52
Figure IV.21: The local and average Sherwood number varied with Ri , for $Le=1, N=1, A=1$ at the left wall.....	52
Figure IV.22: the effect of Aspect ratio on the isocontours while $Le=1, N=1, Ri=1$	54
Figure IV.23: Nusselt number varied with Aspect ratio while $Le=1, N=1, Ri=1$	55
Figure IV.24: Average Nusselt number at different walls varied with Aspect ratio.....	56
Figure IV.25: The local and average Sherwood number varied with Aspect ratio for $Le=1, N=1$, at the left wall.....	56

Tables list:

Table III.1 : Terms of transport equation.....	20
Table III.2 : an explanation for the evaluation of a_E and a_W with different scheme.....	22

Nomenclature:

A	Aspect ratio, H/L
c	mass concentration kg/m^3
c_h	concentrations at the left wall of the cavity
c_c	concentrations at the right wall of the cavity
C	dimensionless concentration, $C=(c-c_c)/(c_h-c_c)$
D	mass diffusivity, m^2/s
g	acceleration of gravity, m/s^2
Gr_S	solulal Grashof number
Gr_T	thermal Grashof number
h	heat transfer coefficient, $\text{W/m}^2\text{K}$
h_S	solulal transfer coefficient, m/s
H	cavity height, m
k	fluid thermal conductivity, W/m K
L	cavity width, m
Le	Lewis number, $Le=\alpha/D=Sc/Pr$
N	buoyancy, Gr_S/Gr_T
Nu_{av}	average Nusselt number, $Nu_{av} = hL/k$
Nu	local Nusselt number
p	pressure, N/m^2
P	dimensionless pressure, $P=p/\rho v_p^2$
Pr	Prandlt number, $Pr=\nu/\alpha$
Re	Reynolds number $Re= v_p L/ \nu$
Ri	Richardson number, $Ri = Gr/Re^2$
Sc	Schmidt number, $Sc= \nu/D$
Sh_{av}	average Sherwood number $Sh_{av} = h_S L/D$
Sh	local Sherwood number
T	local temperature, K
T_c	cold wall temperature, K
T_h	hot wall temperature, K
ΔT	Temperature difference, $\Delta T = T_h - T_c$, K
u	velocity component in x direction
v	velocity component in y direction
U_0	movable plate velocity, m/s
U	dimensionless velocity component in X direction
V	dimensionless velocity component in Y direction
x, y	dimensional coordinates
X, Y	dimensionless coordinates

Greek symbols

α	thermal diffusivity, m^2/s
β_T	coefficient of thermal expansion, K^{-1}
β_S	coefficient of solutal expansion, m^3/kg
θ	dimensionless temperature, $\theta = (T - T_c)/(T_h - T_c)$
μ	dynamic viscosity, $kg/m\ s$
ν	kinematics viscosity, m^2/s
ρ	local fluid density, kg/m^3
ρ_0	characteristic density, kg/m^3

GENERAL INTRODUCTION

General introduction:

The lid driven cavity flow is one of the most studied problems in computational fluid dynamics field. The simplicity of the geometry of the enclosure flow makes the problem easy to code and apply boundary conditions and etc. Even though the problem looks simple in many ways, the flow in a cavity retains all the flow physics with counter rotating vortices appear at the corners of the cavity.

Pure forced convection or pure natural convection situations are very rare at practice. Often the practical process is the mixture of the buoyancy convection and forced convection, and depending on the situations one may predominate over the other. The phenomena of heat and mass transfer are of considerable interest in the field of medicine and engineering. This interest is reflected in human heart, Oil and gas energy, distillation, air conditioning, drying of wood, cooling of electronic components, manufacture of float glass, etc....

In this work, we carry out a numerical study of heat and mass transfer in a rectangular cavity with a movable upper wall. The purpose of the study is to determine the influence of various parameters such as the Richardson number, the buoyancy ratio, the Lewis number and Aspect ratio on the transfer of heat and mass when the fluid is in motion.

This document is organized into five chapters presented below:

We present in the first chapter generalities and a bibliographical analysis which makes it possible to highlight the physical phenomena which must be considered in the case of heat and mass transfers in a cavity.

The chosen physical model, the governing equations as well as the associated boundary conditions constitute the content of the second chapter.

In the third chapter, we present the numerical method used for the resolution of the equations. The systems of algebraic equations obtained associated with the boundary conditions are solved by the use of the TDMA algorithm.

We gather in the fourth chapter the validation of our computer code which is written by the Fortran software as well as the main numerical results of this study and also the comments, interpretations and analyzes of the various results of this study.

Finally, we end with a general conclusion in which are pointed out the particularities of the results obtained in this study.

CHAPTER I:

GENERALITIES

AND LITERATURE REVIEW

I-1-Heat transfer:

I-1-1-Introduction:

On this chapter, we give a brief definition of the heat and mass transfer and other concepts related on this field we used the different books and websites [1-8], and then some reviews of different articles [9-13].

It was clear to people that something flows from hot objects to cold ones, we call that heat flow. But the scientists in the eighteenth and early nineteenth centuries supposed that there is an invisible fluid in all bodies named 'Caloric'. it wasn't correct on some concepts (like heat has a weight) but it was very useful manner to understand that the heat moves from hot to cold bodies.

The life forms have for the human being necessarily evolved to match the magnitude of these energy flows and prevent the loss of it. But while “Caveman” is in balance with these heat flows, “Modern man” has used his mind, his back, and his will to harness and control energy flows that are far more intense than those we experience naturally.

I-1-2-Definition :

Heat transfer (or heat) is thermal energy in transit due to a spatial temperature difference. Heat transfer is the exchange of thermal energy between physical systems. The rate of heat transfer lean on the temperatures of the systems and the properties of the medium through which the heat is transferred through it.

I-1-3-Importance of heat transfer:

The study of heat transfer is applied for the follows purposes:

- 1- To estimate the rate of flow of energy as heat the boundary of a system under studies (both under steady and transient conditions).
- 2- To determine the temperature field for the steady and transient conditions.

In almost every branch of engineering, heat transfer (and mass transfer) are encountered vast areas covered under the discipline of heat transfer:

- *Estimation of thermal and nuclear power plants.
- *Internal combustion engines.
- *Refrigeration and air conditioning units.
- *Design and cooling fluids.

*Construction of dams and structures.

*Heat treatment of metals.

*Dispersion of atmospheric pollutants.

I-1-4-Heat transfer modes:

There is three fundamental modes of heat transfer: conduction, convection and radiation.

I-1-4-1-Conduction:

Fourier's law of heat conduction proves that to estimate the heat transfer through a specific medium of known thermal conductivity and cross-sectional area, one needs the spatial variation of temperature. Farther more the temperature at any point in the System may vary with time also. The spatial and temporal solutions are obtained by solving the heat conduction equation. We can obtain the heat conduction equation by applying first law of thermodynamics and Fourier's law to an elemental control volume of the conducting medium. In rectangular coordinates, the general heat conduction equation for a conducting medium with constant thermal properties (for example heat capacity...) is given by:

$$\frac{1}{\alpha} \frac{\partial T}{\partial t} = \left[\frac{\partial^2 T}{\partial x^2} + \frac{\partial^2 T}{\partial y^2} + \frac{\partial^2 T}{\partial z^2} \right] + \frac{q_g}{k} \quad \text{I-1}$$

In the above equation, $\alpha = \frac{k}{\rho c_p}$ is called as thermal diffusivity, q_g is the rate of heat generation per unit volume inside the control volume, k is the thermal conductivity and t is the time.

The general heat conduction equation given above can be rewritten in a brief form using the Laplacian operator ∇^2

$$\frac{1}{\alpha} \frac{\partial T}{\partial t} = \nabla^2 T + \frac{q_g}{k} \quad \text{I-2}$$

I-1-4-2-Convection:

Convection is the process of heat transfer by bulk movement of molecules within fluids such as gazes and liquids, it involves a bulk transfer of portion of the fluids.

convection and conduction are similar in that mechanism require the presence of medium to transfer the heat from a point to another, on the other they are different

because convection requires the presence of fluid motion but conduction doesn't require it.

I-1-4-2-1-Convection as conduction with fluid motion:

Some experts believe that convection is a special case of thermal conduction, and they did not consider convection as a fundamental mechanism of heat transfer, known as conduction with fluid motion.

I-1-4-2-2-Types of convection:

- Natural convection
- Forced convection
- Mixed convection

A- Natural convection:

when convection takes place due to buoyant force as there is a difference in densities caused by a difference in temperature it is known as natural convection (e.g: Sea breezes).

B-Forced convection:

When the fluid is induced by an external source such as fans or pumps ...this is known as forced convection (e.g: Water heaters..)

C-Mixed convection:

It is the mixture of natural convection and forced convection, it's the most realistic type, almost we can see it in everything in our life.

I-1-4-2-3-Newton's law of cooling:

$$Q = m A \Delta T = m A (T - T_0) \quad \text{I-3}$$

I-1-4-2-3-1- the value of convective heat transfer coefficient h depend on :

- Density
- Viscosity
- Thermal conductivity
- Specific heat capacity

I-1-4-2-4-dimensionless Numbers :

1-Nusselt Number:

The Nusselt Number is a dimensionless number, named after a German engineer willhelm Nusselt, it describe the ratio of the thermal energy conected to the fluid to the thermal energy conducted within the fluid.

$$Nu = \frac{\text{convection heat transfer}}{\text{conduction heat transfer}} = \frac{hL}{k} \quad \text{I-4}$$

2-Reynold Number:

The Reynolds number is the ratio of inertial forces to viscous forces and is a convenient parameter for predicting if a flow condition will be laminar or turbulent.

$$Re = \frac{\text{inertia forces}}{\text{viscous forces}} = \frac{\rho UL}{\mu} = \frac{UL}{\nu} \quad \text{I-5}$$

3- Prandlt Number:

The Prandtl number is a dimensionless number, named after its inventor, a German engineer Ludwig Prandtl. The Prandtl number is defined as the ratio of momentum diffusivity to thermal diffusivity.

$$Pr = \frac{\text{viscous diffusion rate}}{\text{thermal diffusion rate}} = \frac{\nu}{\alpha} = \frac{\mu/\rho}{k/\rho C_p} = \frac{\mu C_p}{k} \quad \text{I-6}$$

4- Grashof Number:

The Grashof number is a dimensionless number, named after Franz Grashof. The Grashof number is defined as the ratio of the buoyant to viscous force acting on a fluid in the velocity boundary layer. Its role in natural convection is much the same as that of the Reynolds number in forced convection.

$$Gr = \frac{\text{bouyant forces}}{\text{viscous forces}} = \frac{g\beta(T-T_0)L^3}{\nu^2} \quad \text{I-7}$$

5-Richrdson Number :

The Richardson number (Ri) is named after Lewis Fry Richardson (1881–1953). It is the dimensionless number that expresses the ratio of the buoyancy term to the flow shear term. Richardson number represents the importance of natural convection relative to the forced convection. The Richardson number in this context is defined as :

$$Ri = \frac{\text{buoyancy term}}{\text{flow shear term}} = \frac{g\beta(T-T_0)L}{v^2} = \frac{Gr}{Re^2} \quad \text{I-8}$$

I-1-4-3- Thermal Radiation:

Is electromagnetic radiation on the infra-red region of electromagnetic spectrum although some of it is in the visible region, it is generated by thermal motion of charged particles in the matter and therefore any material that has temperature above absolute zero gives off some radiant energy.

Thermal Radiation does not require any medium of energy transfer.

Thermal Radiation heat transfer can occur between two bodies separated by medium colder than both bodies.

I-1-4-3- 3-1-Governing Laws:

1-Kirchhoff's Law of Thermal Radiation:

For an arbitrary body emitting and absorbing thermal radiation in thermodynamic equilibrium, the emissivity is equal to the absorptivity.

$$\text{emissivity } \varepsilon = \text{absorptivity } \alpha \quad \text{I-9}$$

As a result of this law, heat cannot spontaneously flow from cold system to hot system and the second law of thermodynamics is still satisfied.

In general, the emissivity, ε , and the absorptivity, α , of a surface depend on the temperature and the wavelength of the radiation. Kirchhoff's law of thermal radiation, postulated by a German physicist Gustav Robert Kirchhoff, states that the emissivity and the absorptivity of a surface at a given temperature and wavelength are equal.

2-Planck's Law:

Planck's law is a pioneering result of modern physics and quantum theory. Planck's hypothesis that energy is radiated and absorbed in discrete "quanta" (or energy packets) precisely matched the observed patterns of blackbody radiation and resolved the ultraviolet catastrophe.

Using this hypothesis, Planck showed that the spectral radiance of a body for frequency ν at absolute temperature T is given by:

$$B(f, T) = \frac{2hf^3}{c^2} \frac{1}{e^{\frac{hf}{k_B T}} - 1} \quad \text{I-10}$$

$B(f,T)$ is the spectral radiance (the power per unit solid angle and per unit of area normal to the propagation) density of frequency ν radiation per unit frequency at thermal equilibrium at temperature T

The Planck's law has the following important features:

- The emitted radiation varies continuously with wavelength.
- At any wavelength the magnitude of the emitted radiation increases with increasing temperature.
- The spectral region in which the radiation is concentrated depends on temperature, with comparatively more radiation appearing at shorter wavelengths as the temperature increases (Wien's Displacement Law).

3-Wien's Displacement Law:

Wien's displacement law (named after a German physicist) describes the shift of that peak in terms of temperature.

Wien's displacement law, and the fact that the frequency is inversely proportional to the wavelength, also indicates that the peak frequency f_{max} (object's color) is proportional to the absolute temperature T of the blackbody.

According to Wien's displacement law, the spectral radiance of black body radiation per unit wavelength, peaks at the wavelength λ_{max} given by:

$$\lambda_{max} = \frac{b}{T} \quad \text{I-11}$$

b is a constant of proportionality, known as Wien's displacement constant, equal to $2.8978 \cdot 10^{-3}$ [K.m].

4-Stefan-Boltzmann Law:

According to the Stefan-Boltzmann law:

Radiation heat transfer rate, q [W/m²], from a body (e.g., a black body) to its surroundings is proportional to the fourth power of the absolute temperature and can be expressed by the following equation:

$$q = \varepsilon \sigma T^4 \quad \text{I-12}$$

where σ is a fundamental physical constant called the Stefan-Boltzmann constant, which is equal to 5.6697×10^{-8} [W/m²K⁴].

I-2-Mass transfer:

I-2-1-Definition:

For system contains two or more components whose concentration vary from here to there, there is a natural way for mass to be transferred, The gradient concentration differences within the system. The transport from a higher concentration to that of lower concentration is called mass transfer. A good example of mass transfer is drying of a wet surface exposed to unsaturated air.

I-2-2-Modes of mass transfer:

There are three different modes of mass transfer: Mass transfer by diffusion, Mass transfer by convection, Mass transfer by change of phase.

I-2-2-1-Mass transfer by diffusion (molecular or eddy diffusion):

The transport of fluid flow on microscopic level as a conclusion of diffusion from a region has higher concentration to a region of lower concentration in a system (or mixture) of liquids or gases is called molecular diffusion. it happens when a substance diffuses through a layer of static fluid may be due to concentration, temperature or pressure gradients. In a gaseous mixture, molecular diffusion occurs due to random motion of the molecules.

If one of the diffusing fluids is in turbulent motion we will get the eddy diffusion .Mass transfer is fast by eddy diffusion than by molecular diffusion.

I-2-2-2-Mass transfer by convection:

Mass transfer by convection requires transfer between a moving fluid and a surface, or between two relatively immiscible moving fluids. The convective mass transfer relies on the transport properties and on the dynamic (laminar or turbulent) characteristics of this fluid.

I-2-2-3-Mass transfer by change of phase:

Mass transfer occurs in the change from one phase to another takes place. The mass transfer in such a case happens due to simultaneous action of convection and diffusion.

I-2-3-Fick's Law:

This law deals with transfer of mass within a medium due to difference in concentration between various parts of it. This is very similar to Fourier's law of heat

conduction as the mass transport is also by molecular diffusion processes. According to this law, rate of diffusion (kg/s) is proportional to the concentration gradient and the area of mass transfer:

$$\dot{m} = -DA \frac{dc}{dx} \quad \text{I-13}$$

where, D is called diffusion coefficient, and it has the units of m²/s just like those of thermal diffusivity α and the kinematic viscosity of fluid ν for momentum transfer.

I-2-4-General equation of mass transfer :

$$\frac{Dc}{Dt} = D\Delta c + \dot{N}_A \quad \text{I-14}$$

Where \dot{N}_A is the molar rate of production.

I-2-5-Dimensionless Numbers :

1-Sherwood Number:

The Sherwood number is a dimensionless number, named after Thomas Kilgore Sherwood. The Sherwood number is defined as the ratio of the convective mass transfer to the mass diffusivity.

$$Sh = \frac{\text{convective mass transfer}}{\text{mass diffusion rate}} = \frac{h_m}{D/L} \quad \text{I-15}$$

The number of Sherwood in mass transfer correspondent to Nusselt number in heat transfer.

2-Schmidt Number:

The Schmidt number is a dimensionless number, named after the German engineer Ernst Heinrich Wilhelm Schmidt (1892–1975). The Schmidt number is defined as the ratio of momentum diffusivity (kinematic viscosity) and mass diffusivity, and is used to characterize fluid flows in which there are simultaneous momentum and mass diffusion convection processes. The Schmidt number describes the mass momentum transfer, and the equations can be seen below:

$$Sc = \frac{\text{viscous diffusion rate}}{\text{mass diffusion rate}} = \frac{\nu}{D} = \frac{\mu}{\rho D} \quad \text{I-16}$$

3-Lewis Number:

The Lewis number is a dimensionless number, named after Warren K. Lewis (1882–1975). The Lewis number is defined as the ratio of thermal diffusivity and mass

diffusivity. It is used to characterize fluid flows where there is simultaneous heat and mass transfer. The Lewis number is therefore a measure of the relative thermal and concentration boundary layer thicknesses. The Lewis number can also be expressed in terms of the Prandtl number and the Schmidt number as $Le = Sc / Pr$.

$$Le = \frac{\text{Thermal diffusion rate}}{\text{mass diffusion rate}} = \frac{\alpha}{D} \quad \text{I-17}$$

4-Buoyancy ratio :

It is non dimensional number that expresses the ratio of solutal convection to thermal convection.

$$N = \frac{Gr_S}{Gr_T} \quad \text{I-18}$$

I-3-Reviews :

A.M. Al-Amiri et al. [9] presented a numerical study of stationary mixed convection in a moving-wall cavity under the effect of the combination of thermal diffusion and mass diffusion. Heat and mass transfer were examined with the use of several dimensionless parameters such as Richardson number, Lewis number and buoyancy ratio. The physical model imposed for this reference is the side wall (vertical walls) are adiabatic and impermeable while the horizontal walls is uniformly concentrated and heated but the bottom is hotter and more concentrated.

Mohamed A. Teamah a, Wael M. El-Maghlany b [10],The present study deals with mixed convection in a rectangular lid-driven cavity under the combined buoyancy effects of thermal and mass diffusion. Convective flux with double diffusion in a rectangular enclosure with movable upper surface is studied numerically. The top and bottom surfaces are being insulated and waterproof. Constant temperatures and concentrations are imposed along the vertical walls of the enclosure, a laminar regime is considered in the state of equilibrium. The transport equations for continuity, momentum, energy and spice transfer are solved. Numerical results are reported for the effect of Richardson number, Lewis number and coefficient of buoyancy on the streamline, temperature and concentration. In addition, predicted results for Nusselt and local means and mean Sherwood numbers are presented and discussed for various parametric conditions. This study was made for $0.1 < Le < 50$ and Prandtl number $Pr=0.7$. Throughout the study, the number and format of the Grashof image are kept constant, whereas the Richardson number was changed from 0.01 to 10 to simulate a flow dominated by forced convection, mixed convection and flux dominated natural convection.

Mefteh Bouhalleb AND Hassan Abbassi [11],Two-dimensional stable laminar natural convection in an inclined rectangular enclosure filled with CuOewater

nanofluid is investigated numerically. The horizontal walls are thermally insulated and the left vertical side wall is heated by a spatial temperature distribution. The mass, momentum and energy conservation equations are solved numerically by the volume finite element method using the SIMPLER algorithm for rotational speed coupling. This study was carried out for the relevant parameters in the following areas: ranges: angle of inclination, the volumetric fraction of the nanoparticles between 0 and 4% and aspect ratio. These simulations are performed at constant Rayleigh and Prandtl numbers, they are fixed at Ra and Pr . The results are presented in the form of streamlines, isotherms and Nusselt numbers. Heat transfer increases first, then decreases with enclosure tilt for aspect ratio and increases with increasing tilt angle for $Ar < 1$. The rate of heat transfer increases with increasing volume fraction of nanoparticles. The subject of this article is to study the effect of nanoparticles on heat transfer, as well as the effect of tilt angle and aspect ratio.

M. Sathiyamoorthy a, Tanmay Basak b, S. Roy c, I. Pop d,* [12] The present numerical study deals with the natural convection flow in a square closed cavity when the bottom wall is heated uniformly and the vertical wall(s) are heated linearly, while the top wall is well insulated. Nonlinear coupled PDEs governing the flow have been solved by the finite element method with bi-quadratic rectangular elements. Numerical results are obtained for different values of Rayleigh number (Ra) and Prandtl number (Pr). The results are presented as streamlines, isothermal contours, local Nusselt number and mean Nusselt as a function of Rayleigh number.

Youssef Stiriba [13] A numerical study was performed to analyze the effects of mixed convective auxiliary flow beyond a three-dimensional open cavity over a wide range of Reynolds (100 to 1000) and Richardson (0.001 to 10) numbers. The vertical walls in the inlet and outlet sides are isothermal while all other walls are adiabatic. The cavity is assumed to be of cubic geometry and the flow is laminar. A direct numerical simulation is undertaken to study the flow structure, the heat transfer characteristics and the complex interaction between induced flux at room temperature and flux induced by the buoyancy of the heated wall. It is found that the flow becomes stable at a moderate Grashof number and exhibits a three-dimensional structure, while for a high Richardson number mixed convection effects come into play and push the zone recirculation system further upstream and the flow may become unstable.

Conclusion:

After this generality and the different published scientific articles we gain an acceptable knowledge about Heat and mass transfer its mechanism and the significant of dimensionless parameters to have a better start to treat the present problem.

CHAPTER II:

PROBLEM DESCRIPTION

AND MATHEMATICAL

FORMULATION

II-1-Introduction :

In this chapter, we will expose the studied problem, and we will start by describing the geometry of the physical system and also Mathematical formulation of the governing equations of the present problem.

Finally, the boundary and initial conditions are depicted and presented to give a general identifying of the problem.

II-2-Problem formulation:

A schematic diagram of a two-dimensional rectangular cavity is displayed in Figure II.1 where the bottom wall is maintained at a uniform temperature. Side walls are kept linearly heated the top wall is well insulated. The top wall is assumed to slide from left to right with constant speed U_0 . constant different concentration are imposed at the vertical walls while the horizontal wall are impermeable .the thermophysical properties of the fluid such as viscosity,thermal conductivity,specific heats,thermal expansion coefficient except the density variation in the buoyancy term are considered to be constant.The Boussinesq approximation is considered for the body force term involving the variation of density of fluid with temperature and to couple the temperature and mass fields to the flow field.

The heat and mass transfer occurs by mixed convection where the fluid excited by the lid driven, thermal forces and mass forces.

The solution of this problem depends on the governing equations which are mass conservation, momentum equation, energy and concentration equations.

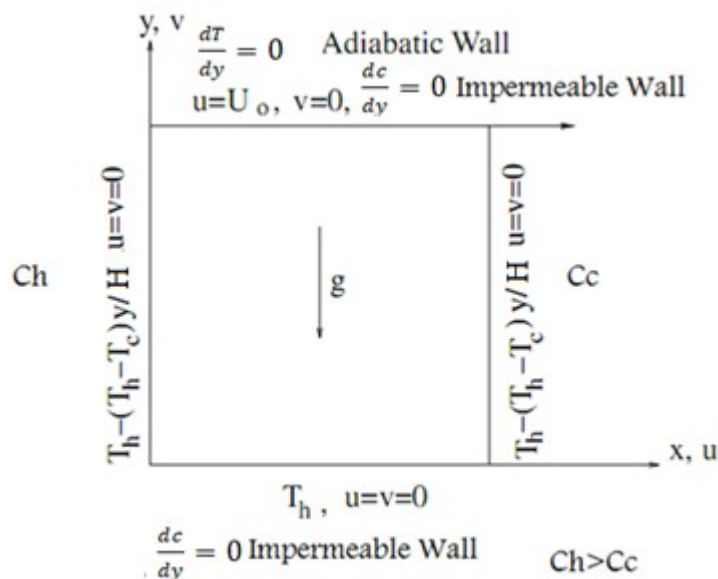


Figure II.1 a schematic physical model

II-3-Hypotheses:

For simplifying the current present work we took this following hypothesis to work with an ease:

- The bidimensional problem
- Steady state flow
- Laminar flow
- Newtonien fluid, viscous and incompressible

II-4-Mathelatical formulation :

The governing equations of mass conservation, momentum equations, concentration and energy equation are for the mixed convection laminar and steady state flows inside the cavity.

II-4-1-Mass conservation:

$$\frac{\partial u}{\partial x} + \frac{\partial v}{\partial y} = 0 \quad \text{II.1}$$

II-4-2-Momentum equation:

For U velocity (projection in ox Label)

$$\left(u \frac{\partial u}{\partial x} + v \frac{\partial u}{\partial y} \right) = -\frac{1}{\rho} \frac{\partial P}{\partial x} + \vartheta \left(\frac{\partial^2 u}{\partial x^2} + \frac{\partial^2 u}{\partial y^2} \right) \quad \text{II.2}$$

For V velocity (projection in oy label)

$$\left(u \frac{\partial v}{\partial x} + v \frac{\partial v}{\partial y} \right) = -\frac{1}{\rho} \frac{\partial P}{\partial y} + \vartheta \left(\frac{\partial^2 v}{\partial x^2} + \frac{\partial^2 v}{\partial y^2} \right) + g[\beta_T(T - T_C) - \beta_S(c - c_C)] \quad \text{II.3}$$

II-4-3-Energie equation :

$$\left(u \frac{\partial T}{\partial x} + v \frac{\partial T}{\partial y} \right) = \alpha \left(\frac{\partial^2 T}{\partial x^2} + \frac{\partial^2 T}{\partial y^2} \right) \quad \text{II.4}$$

II-4-4-Concentration equation :

$$\left(u \frac{\partial c}{\partial x} + v \frac{\partial c}{\partial y} \right) = D \left(\frac{\partial^2 c}{\partial x^2} + \frac{\partial^2 c}{\partial y^2} \right) \quad \text{II.5}$$

II-5-Boundary conditions :

The boundary conditions of the present work are:

For velocities:

Left wall: for $x = 0$; $0 \leq y \leq H$; $u = 0, v = 0$

Right wall: for $x = L$; $0 \leq y \leq H$; $u = 0, v = 0$

Top wall: for $y = H$; $0 \leq x \leq L$; $u = U_0, v = 0$

Bottom wall: for $y = 0$; $0 \leq x \leq L$; $u = 0, v = 0$

For temperature:

Left wall: for $x = 0$; $0 \leq y \leq H$; $T = T_h - (T_h - T_c) \frac{y}{H}$

Right wall: for $x = L$; $0 \leq y \leq H$; $T = T_h - (T_h - T_c) \frac{y}{H}$

Top wall: for $y = H$; $0 \leq x \leq L$; $\frac{dT}{dy} = 0$

Bottom wall: for $y = 0$; $0 \leq x \leq L$; $T = T_h$

For concentration:

Left wall: for $x = 0$; $0 \leq y \leq H$; $c = c_h$

Right wall: for $x = L$; $0 \leq y \leq H$; $c = c_c$

Top wall: for $y = H$; $0 \leq x \leq L$; $\frac{dc}{dy} = 0$

Bottom wall: for $y = 0$; $0 \leq x \leq L$; $\frac{dc}{dy} = 0$

II-6-Dimensionless groups :

$$X = \frac{x}{L}; Y = \frac{y}{L}; U = \frac{u}{U_0}; V = \frac{v}{U_0}; P = \frac{p}{\rho U_0^2}; \theta = \frac{T - T_c}{T_h - T_c}; C = \frac{c - c_c}{c_h - c_c}$$

II-7-Dimensionless governing equations:

$$\frac{\partial U}{\partial X} + \frac{\partial V}{\partial Y} = 0 \quad \text{II.6}$$

$$\left(U \frac{\partial U}{\partial X} + V \frac{\partial U}{\partial Y} \right) = - \frac{\partial P}{\partial X} + \frac{1}{Re} \left(\frac{\partial^2 U}{\partial x^2} + \frac{\partial^2 U}{\partial y^2} \right) \quad \text{II.7}$$

$$\left(U \frac{\partial V}{\partial X} + V \frac{\partial V}{\partial Y} \right) = - \frac{\partial P}{\partial Y} + \frac{1}{Re} \left(\frac{\partial^2 V}{\partial X^2} + \frac{\partial^2 V}{\partial Y^2} \right) + \frac{Gr}{Re^2} (\theta + NC) \quad \text{II.8}$$

$$\left(U \frac{\partial \theta}{\partial X} + V \frac{\partial \theta}{\partial Y} \right) = \frac{1}{RePr} \left(\frac{\partial^2 \theta}{\partial X^2} + \frac{\partial^2 \theta}{\partial Y^2} \right) \quad \text{II.9}$$

$$\left(U \frac{\partial C}{\partial X} + V \frac{\partial C}{\partial Y} \right) = \frac{1}{LeRePr} \left(\frac{\partial^2 C}{\partial X^2} + \frac{\partial^2 C}{\partial Y^2} \right) \quad \text{II.10}$$

$$N = \frac{Gr_S}{Gr_T}$$

II-8-Dimensionless boundary condition:

Vertical boundaries:

$$U=V=0 ; \theta = 1 - Y \text{ and } C = 1 \text{ at } X = 0$$

$$U=V=0 ; \theta = 1 - Y \text{ and } C = 0 \text{ at } X = 1$$

Horizontal boundaries:

$$U=V=0 ; \theta = 1 \text{ and } \frac{dC}{dY} = 0 \text{ At } Y = 0$$

$$V=0 ; \frac{d\theta}{dY} = 0 \text{ and } \frac{dC}{dY} = 0 \text{ and } U = 1 \text{ At } Y = \frac{H}{L}$$

II-9-Nusselt number: the local and the average Nusselt number at the left bottom and right walls respectively

$$Nu_{Left\ wall} = -\left(\frac{\partial \theta}{\partial X}\right)_{X=0} \quad Nu_{Bottom\ wall} = -\left(\frac{\partial \theta}{\partial Y}\right)_{Y=0} \quad Nu_{Right\ wall} = -\left(\frac{\partial \theta}{\partial X}\right)_{X=L}$$

$$Nu_{av-L} = -\frac{1}{A} \int_0^A \left(\frac{\partial \theta}{\partial X}\right)_{X=0} dY \quad Nu_{av-B} = -\int_0^1 \left(\frac{\partial \theta}{\partial Y}\right)_{Y=0} dX \quad Nu_{av-RW} = -\frac{1}{A} \int_0^A \left(\frac{\partial \theta}{\partial X}\right)_{X=L} dY$$

II-10-Sherwood number: the local and the average Sherwood number at the left wall:

$$Sh_{Left\ wall} = -\left(\frac{\partial C}{\partial X}\right)_{X=0} ; Sh_{av-L} = -\frac{1}{A} \int_0^A \left(\frac{\partial C}{\partial X}\right)_{X=0} dY$$

II-11-The stream function :

$$U = \frac{\partial \psi}{\partial Y} ; V = -\frac{\partial \psi}{\partial X}$$

II-12-Conclusion :

In this chapter, the governing equations used to solve the mixed double diffusive convection problem in a rectangular cavity filled by incompressible fluid, represented in both forms :dimensional and non dimensional equations for the reason to show up the different dimensionless numbers like Ri,Le,N..

CHAPTER III :

RESOLUTION METHOD

III-1-Introduction:

As we know there is three major methods used to discretize the Partial differential equations to get a close approximation (Or to be more precise an approach solution) to avoid the complexity of analytical solution which it has a lot of cases without solution for example :there is no Analytical solution for the complete form of Navier-Stokes equation -it is also called the momentum equation- for the three dimensions, even this solution (Analytical solution) is more accurate than numerical method but it is so recommended to use an approximations to reduces time and get the solutions with ease and an additional factor confirm to choose numerical solution is the bulk development of computers which it becomes a very fast to treat a huge amount of calculations so we can rely on it in condition we are following a the correct instructions to the solution (For example developing an algorithm with Matlab to solve Navier-Stokes equations with of course taking in consideration the right implementation of the boundary conditions ,initial condition, the algorithm followed :SIMPLE,SIMPLER,SIMPLEC) or using directly Software to get the solution : ANSYS,COMSOL....

Those three major methods are:

*Finite volume method

*Finite element method

*Finite differencing method

In our case we will treat our problem with the Finite Volume Method (FVM) which is the best option for Computational Fluid Dynamics (CFD) and it fit the boundary and initial condition for fluid flow more than the other two methods so we expect a better convergence and on fast manner.

But if we want to class the previous methods from harder to easier we will find the finite Element Method is the hardest and the Finite differencing method is easier one while our option is not too complicated nor too Simple and this also another advantage that encourage us to work with method.

With MVF we can discretize all kind of governing equation: (forced or natural convection) on momentum equations, Scalar equation (Temperature , concentration..) and discretising the boundary conditions and also velocities and pressure for initial conditions and for Temperature and concentration for solution process.

III-2-Transport equation :

The transport equation describes how a physical scalar is transported (or flows) in a space. Therefore its applied for transport phenomena like (Temperature, Concentration ...) inside a specific volume called control volume. For Mathematical formulation of this transport equation its about a first order partial differential equation (PDE) it's also known as convection-diffusion equation which is generalized to represent the most common transportation model.[14]

$$\frac{\partial \rho \phi}{\partial t} + \nabla \rho U \phi = \Delta \Gamma \phi + S \quad \text{III.1}$$



III-3-Staggered grid :[5]

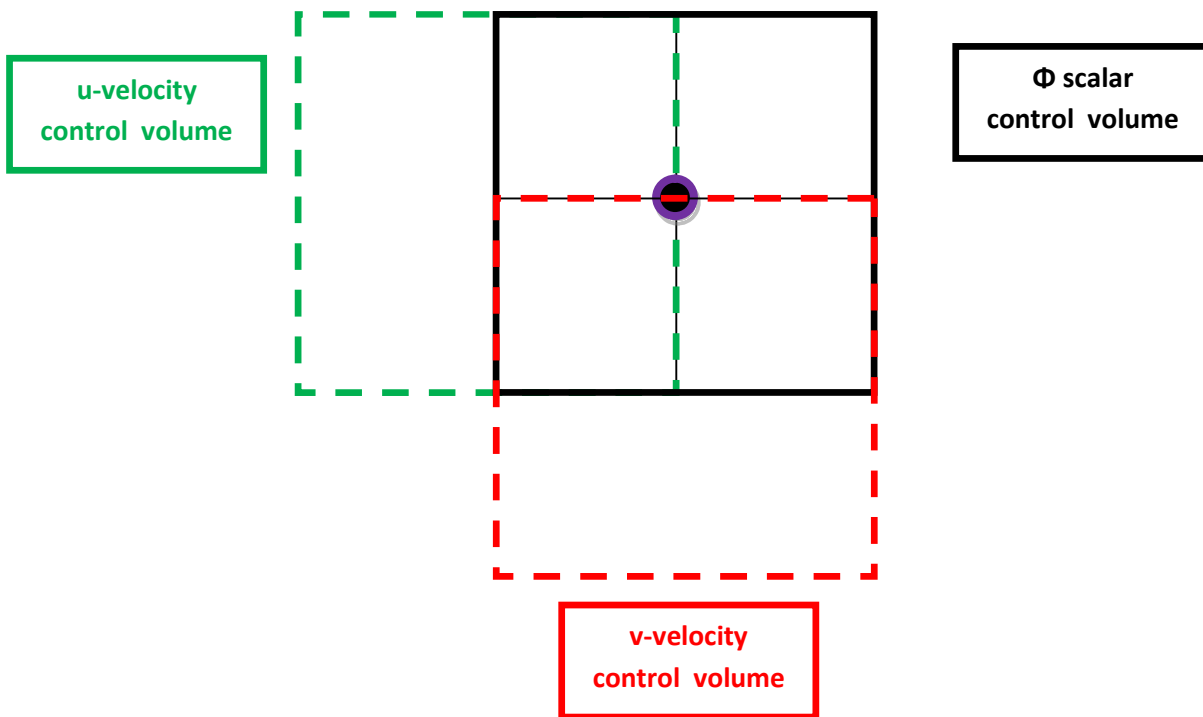


Figure III.1: Staggered grid schema

Staggered grid is one of the most important parts for the solution procedure hence we could not ignore this step.

As we know the finite volume method starts as always with the discretisation of flow domain and also the transport equation.

Staggered grid lead us to estimate velocities situated on the centered cell faces but to store the scalar variable (pressure, temperature, concentration...) at the ordinary control

volume, so we conclude that the control volume of u and v are different from the scalar control volume and from each other too.

The staggering of the velocity avoids the unrealistic behavior of the discretised momentum equation for spatially oscillating pressure so a high non-uniform pressure field will act like a uniform field in the discretised momentum equation if we don't use this technique.

III-4-The central differential scheme :

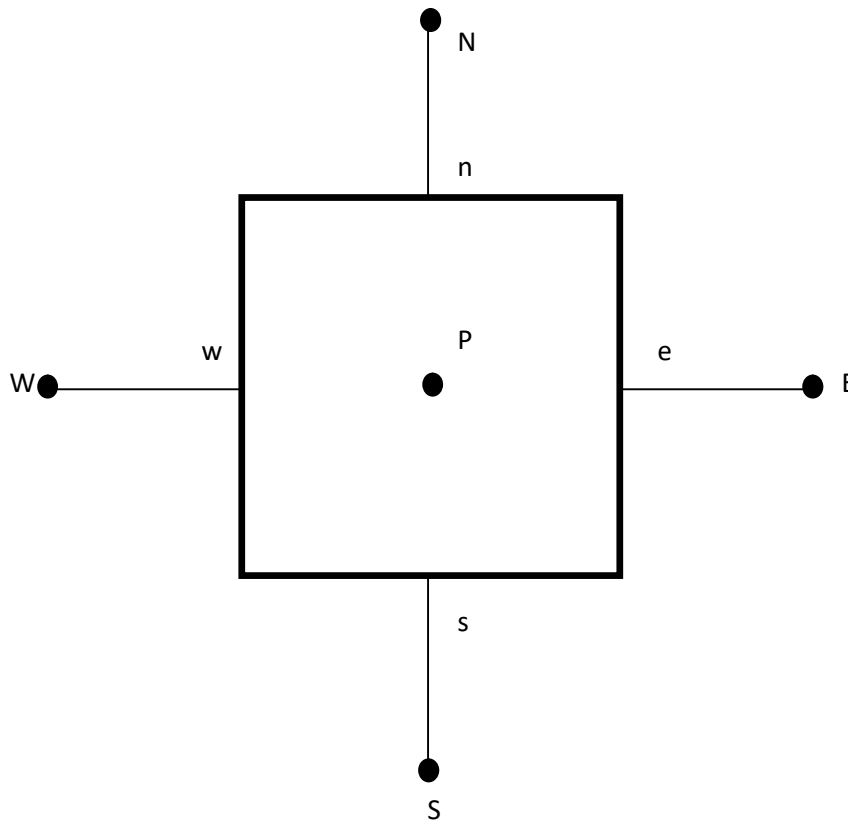


Figure III.2: central differential scheme

Central differencing approximation has been used to represent the diffusion term which appear on the right hand side of transport equation and it seems logical to try linear interpolation to compute the cell face values for convective terms on the left side of the same equation.

$$\phi_e = \frac{\phi_P + \phi_E}{2} ; \phi_w = \frac{\phi_P + \phi_W}{2} ; \phi_n = \frac{\phi_P + \phi_N}{2} ; \phi_s = \frac{\phi_P + \phi_S}{2} \quad \text{III.2}$$

III-5-Discretisation of transport equation: [5]

We will work with the steady state 2D dimension problem

$$\underbrace{\nabla \rho U \phi}_{\text{Convection}} = \underbrace{\Delta \Gamma \phi}_{\text{Diffusion}} + \underbrace{S}_{\text{Source term}} \quad \text{III.3}$$

The following table introduces to us some of variables with their terms forming a specific equation

Table III.1: Terms of transport equation

Equations	The variable	The diffusion term	The Source term
Continuity	1	0	0
X momentum	U	$\frac{1}{Re}$	$-\frac{\partial P}{\partial X}$
Y momentum	V	$\frac{1}{Re}$	$-\frac{\partial P}{\partial Y} + \frac{G_r}{Re^2}(\theta + NC)$
Energy	Θ	$\frac{1}{RePr}$	0
Concentration	C	$\frac{1}{RePrLe}$	0

-By integration the equation (III.3) over a control volume (cv) gives :

$$\int_{cv} \nabla U \phi \, dx dy = \int_{cv} \Delta \Gamma \phi \, dx dy + \int_{cv} S \, dv \quad \text{III.4}$$

With the theory of Ostogradski we will get:

$$\underbrace{\int_{cs} U \phi \, dx dy}_{(1)} = \underbrace{\int_{cs} \Gamma \text{grad} \phi \, dx dy}_{(2)} + \underbrace{\int_{cv} S \, dv}_{(3)} \quad \text{III.5}$$

$$\begin{aligned} (1) \quad : \int_{cs} U \phi \, dx dy &= \int_w^e \int_s^n U \phi \, dX dY \\ &= ((U\phi)_e - (U\phi)_w) \Delta y + ((V\phi)_n - (V\phi)_s) \Delta X \end{aligned} \quad \text{III.6}$$

$$\begin{aligned} (2) \quad : \int_{cs} \Gamma \text{grad} \phi \, dx dy &= \int_w^e \int_s^n \Gamma \left[\left(\frac{\partial \phi}{\partial X} \right) + \left(\frac{\partial \phi}{\partial Y} \right) \right] dX dY \\ &= \Gamma \left[\left(\left(\frac{\partial \phi}{\partial X} \right)_e - \left(\frac{\partial \phi}{\partial X} \right)_w \right) \Delta Y + \left(\left(\frac{\partial \phi}{\partial Y} \right)_n - \left(\frac{\partial \phi}{\partial Y} \right)_s \right) \Delta X \right] \end{aligned} \quad \text{III.7}$$

$$(3) : \int_{cv} S dv = \int_w^e \int_s^n S dx dy = \bar{S} \Delta x \Delta y = (S_u + S_p \phi_p) \Delta x \Delta y \quad \text{III.8}$$

For evaluation $\phi_e, \phi_w, \phi_n, \phi_s$, we use central differencing scheme :

$$\begin{aligned} \phi_e &= \frac{\phi_E + \phi_P}{2} \\ \phi_w &= \frac{\phi_W + \phi_P}{2} \\ \phi_n &= \frac{\phi_N + \phi_P}{2} \\ \phi_s &= \frac{\phi_S + \phi_P}{2} \end{aligned} \quad \text{III.9}$$

We do the same thing for : $\left(\frac{\partial \phi}{\partial X}\right)_e, \left(\frac{\partial \phi}{\partial X}\right)_w, \left(\frac{\partial \phi}{\partial Y}\right)_n, \left(\frac{\partial \phi}{\partial Y}\right)_s$

$$\begin{aligned} \left(\frac{\partial \phi}{\partial X}\right)_e &= \frac{\phi_E - \phi_P}{\Delta X_e}; \\ \left(\frac{\partial \phi}{\partial X}\right)_w &= \frac{\phi_P - \phi_W}{\Delta X_w}; \\ \left(\frac{\partial \phi}{\partial Y}\right)_n &= \frac{\phi_N - \phi_P}{\Delta Y_n}; \\ \left(\frac{\partial \phi}{\partial Y}\right)_s &= \frac{\phi_P - \phi_S}{\Delta Y_s}; \end{aligned} \quad \text{III.10}$$

We sum up all the previous relations into the original equation (III.5):

$$\begin{aligned} \bullet \quad & \left[u_e \frac{\phi_E + \phi_P}{2} - u_w \frac{\phi_W + \phi_P}{2} \right] \Delta y + \left[v_n \frac{\phi_N + \phi_P}{2} - v_s \frac{\phi_S + \phi_P}{2} \right] \Delta x = \left[\Gamma_e \frac{\phi_E}{\delta x_e} - \Gamma_e \frac{\phi_P}{\delta x_e} - \left(-\Gamma_w \frac{\phi_W}{\delta x_w} + \Gamma_w \frac{\phi_P}{\delta x_w} \right) \right] \Delta y + \\ & \left[\Gamma_n \frac{\phi_N}{\delta x_n} - \Gamma_n \frac{\phi_P}{\delta x_n} - \left(-\Gamma_s \frac{\phi_S}{\delta x_s} + \Gamma_s \frac{\phi_P}{\delta x_s} \right) \right] \Delta x + (S_u + S_p \phi_p) \Delta x \Delta y \end{aligned} \quad \text{III.11}$$

$$\begin{aligned} \bullet \quad & \phi_p \left[\left(\frac{u_e - u_w}{2} \right) \Delta y + \left(\frac{v_n - v_s}{2} \right) \Delta x + \left(\frac{\Gamma_e}{\delta x_e} + \frac{\Gamma_w}{\delta x_w} \right) \Delta y + \left(\frac{\Gamma_n}{\delta y_n} + \frac{\Gamma_s}{\delta y_s} \right) \Delta x - \right. \\ & \left. S_p \Delta x \Delta y \right] = \phi_E \left[\left(\frac{\Gamma_e}{\delta x_e} - \frac{u_e}{2} \right) \Delta y \right] + \phi_W \left[\left(\frac{\Gamma_w}{\delta x_w} + \frac{u_w}{2} \right) \Delta y \right] + \phi_N \left[\left(\frac{\Gamma_n}{\delta y_n} - \frac{v_n}{2} \right) \Delta x \right] + \\ & \phi_S \left[\left(\frac{\Gamma_s}{\delta y_s} - \frac{v_s}{2} \right) \Delta x \right] + S_u \Delta x \Delta y \end{aligned} \quad \text{III.12}$$

• by matching the equation (III.12) and :

$$a_p \phi_p = a_E \phi_E + a_W \phi_W + a_N \phi_N + a_S \phi_S + b$$

& if we pose that $F_i = u_i \Delta i$ and $D_i = \frac{\Gamma_i}{\delta i} \Delta j$

We will found that :

$$a_E = \left(\frac{\Gamma_e}{\delta x_e} - \frac{u_e}{2} \right) \Delta y ; a_W = \left(\frac{\Gamma_w}{\delta x_w} + \frac{u_w}{2} \right) \Delta y ;$$

$$a_N = \left(\frac{\Gamma_n}{\delta y_n} - \frac{v_n}{2} \right) \Delta x ; a_S = \left(\frac{\Gamma_s}{\delta y_s} + \frac{v_s}{2} \right) \Delta x ;$$

$$a_P = a_E + a_W + a_N + a_S + F_e - F_w + F_n - F_s \quad \text{III.13}$$

III-6-The discretisation schemes :

Table III.2 : an explanation for the evaluation of a_E and a_W with different schemes

Schéma	a_E	a_W
Central	$a_E = D_e - \frac{F_e}{2}$	$a_W = D_w + \frac{F_w}{2}$
Upwind	$a_E = D_e + [-F_e, 0]$	$a_W = D_w + [-F_w, 0]$
Exponential	$a_E = \frac{F_e}{\exp(P_e) - 1}$	$a_W = \frac{F_w \exp(P_w)}{\exp(P_w) - 1}$
Hybride	$a_E = \left[-F_e, D_e - \frac{F_e}{2}, 0 \right]$	$a_W = \left[-F_w, D_w + \frac{F_w}{2}, 0 \right]$
Power law	$a_E = D_e \left[0, \left(1 - \frac{0.1 F_e }{D_e} \right)^5 \right] + [0, -F_e]$	$a_W = D_w \left[0, \left(1 - \frac{0.1 F_w }{D_w} \right)^5 \right] + [0, F_w]$

For more accuracy and to get better results we need to use advanced schemes for example power law to ensure the convergence to the exact solution for the discretized equation. Because the normal discretized scheme which is central differential scheme does not take in consideration the flow Direction or Pe Peclic number on consideration even they are so linked with physical phenomena which may result catastrophe for the solution and give unrealistic values for different scalars.

For this reason we will rely on the power law scheme for our discretisation process to evaluate the coefficients a_P, a_E, a_W, a_N and a_S

III-7-Implementation of boundary conditions :[5]

III-7-1-Wall boundary conditions :

The wall is the most common boundary encountered in confined fluid flow problems (cavity).

III-7-2-Laminar Flow / Linear sub-layer:

The wall shear stress is obtained from $\tau_w = \mu \frac{u_p}{\Delta y_p}$ III.14

The wall shear forces is given by : $F_s = -\tau_w A_{cell} = \mu \frac{u_p}{\Delta y_p} A_{cell}$ III.15

*The appropriate source term in the u-equation is defined by: $S_p = -\frac{\mu}{\Delta y_p} A_{cell}$ III.16

Heat transfer from a wall at fixed temperature T_w into the new wall cell in a laminar flow is calculated from: $q_s = -\frac{\mu C_p (T_p - T_w)}{\sigma \Delta y_p} A_{cell}$ III.17

With: C_p : the specific heat ; σ : laminar Prandlt number

* $S_p = -\frac{\mu C_p}{\sigma \Delta y_p}$ and $S_u = \frac{\mu C_p T_w}{\sigma \Delta y_p}$ III.18

$q_s = S_u + S_p T_p$ III.19

For adiabatic wall : $S_u = S_p = 0$

III-7-3-Moving wall:

$F_s = \mu \frac{C_p (u_p - u_{wall})}{\Delta y_p} A_{cell}$ III.20

$S_p = -\frac{\mu}{\Delta y_p}$ III.21

$S_u = \frac{\mu}{\Delta y_p} u_{wall}$ III.22

III-8-Solution of discretized equation :

The discretising of the governing equation of fluid flow (or heat transfer or both) yields us to solve a system of linear algebraic equations. There are two families of solution technique for linear algebraic equation: The direct method and the iterative (indirect) method. The iterative methods are much more economical than direct method.

Jacobi and Gauss-Seidel iterative methods are easy to implement in simple computer programs, but they can be slow to converge when the system of equation is large. Hence they are not considered suitable for general CFD procedures. Thomas (1949) developed a technique for rapidly solving tri-diagonal systems that is now called Thomas algorithm or tri-diagonal matrix algorithm (TDMA). This method is actually a direct method for one dimensional situation, but it can be applied iteratively in a line by line fashion, to solve multi dimensional problems and is widely used in CFD programs. It is computationally inexpensive and has the advantage that it requires a minimum amount of storage.

III-8-1-TDMA Algorithm :

$$\begin{aligned}
 \phi_1 &= C_1 \\
 -\beta_2\phi_1 + D_2\phi_2 - \alpha_2\phi_3 &= C_2 \\
 -\beta_3\phi_2 + D_3\phi_3 - \alpha_3\phi_4 &= C_3 \\
 -\beta_4\phi_3 + D_4\phi_4 - \alpha_4\phi_5 &= C_4 \quad \text{III.23} \\
 \dots & \dots \\
 -\beta_n\phi_{n-1} + D_n\phi_n - \alpha_n\phi_{n+1} &= C_n \\
 \phi_{n+1} &= C_{n+1}
 \end{aligned}$$

The unknown equations can be rewritten as:

$$\begin{aligned}
 \phi_2 &= \frac{\alpha_2}{D_2}\phi_3 + \frac{\beta_2}{D_2}\phi_1 + \frac{C_2}{D_2} \\
 \phi_3 &= \frac{\alpha_3}{D_3}\phi_4 + \frac{\beta_3}{D_3}\phi_2 + \frac{C_3}{D_3} \\
 \phi_4 &= \frac{\alpha_4}{D_4}\phi_5 + \frac{\beta_4}{D_4}\phi_2 + \frac{C_4}{D_4}
 \end{aligned}$$

$$\phi_n = \frac{\alpha_n}{D_n} \phi_{n+1} + \frac{\beta_n}{D_n} \phi_{n-1} + \frac{C_n}{D_n} \quad \text{III.24}$$

For back substitution we use the general form of recurrence relationship :

$$\phi_j = A_j \phi_{j+1} + C'_j \quad \text{III.25}$$

Where :

$$A_j = \frac{\alpha_j}{D_j - \beta_j A_{j-1}} \quad \text{III.26}$$

$$C'_j = \frac{\beta_j C'_{j-1} + C_j}{D_j - \beta_j A_{j-1}} \quad \text{III.27}$$

With :

$$C'_1 = \phi_1; A_1 = 0$$

$$C'_{n+1} = \phi_{n+1}; A_{n+1} = 0$$

In order to solve a system of equations it is first to arrange in the form of equations (tri-diagonal) and α_j, β_j, C'_j are identified, the values of A_j and C'_j are subsequently calculated starting at $j=2$ and going up to $j=n$. Since the value of ϕ is known at boundary location (1) and (n+1) the values of ϕ_j can be obtained in reverse order by mean of recurrence formula the is simple and easy to incorporate into CFD program

III-9-SIMPLE Algorithm :[4][5]

The acronym SIMPLE stands for Semi-Implicit method for Pressure-Linked Equations and its created and developed by Patanckar [4].

To initiate the SIMPLE calculation process a pressure field P^ is guessed.

Discretized momentum equations are solved using the guessed pressure filed to yield velocity components u^ and v^* as follows :

$$a_{i,j} u^*_{i,j} = \sum a_{nb} u^*_{nb} + (P^*_{I-1,J} - P^*_{I,J}) A_{I,J} + \bar{S} \Delta V_u \quad \text{III.14}$$

$$a_{i,j} v^*_{i,j} = \sum a_{nb} v^*_{nb} + (P^*_{I-1,J} - P^*_{I,J}) A_{I,J} + \bar{S} \Delta V_v \quad \text{III.15}$$

* P' is the difference between the correct pressure field P and the guessed pressure field P^* .

$$P = P^* + P' \quad \text{III.16}$$

Similarly for u' and v'

$$u = u^* + u' \quad \text{III.17}$$

$$v = v^* + v' \quad \text{III.18}$$

Substitution of the correct pressure velocities field from guessed pressure ,velocities filed :

$$a_{i,j}(u_{i,j} - u^*_{i,j}) = \sum a_{nb}(u_{nb} - u^*_{nb}) + ((P_{I-1,J} - P^*_{I-1,J}) - (P_{I-1,J} - P^*_{I,J}))A_{I,J} \quad \text{II.19}$$

$$a_{I,j}(v_{I,j} - v^*_{I,j}) = \sum a_{nb}(v_{nb} - v^*_{nb}) + ((P_{I-1,J} - P^*_{I-1,J}) - (P_{I-1,J} - P^*_{I,J}))A_{I,J} \quad \text{III.20}$$

So :

$$a_{i,j}u'_{i,j} = \sum a_{nb}u'_{i,j} + (P'_{I-1,J} - P'_{I,J})A_{I,J} \quad \text{III.21}$$

$$a_{I,j}v'_{I,j} = \sum a_{nb}v'_{I,j} + (P'_{I-1,J} - P'_{I,J})A_{I,J} \quad \text{III.22}$$

At this point an approximation is introduced $\sum a_{nb}u'_{i,j}$ and $\sum a_{nb}v'_{I,j}$ are eliminated, The omission of these terms is the main approximation of the SIMPLE algorithm. :

$$\begin{cases} u'_{i,j} = d_{i,j}(P'_{I-1,J} - P'_{I,J}) \\ v'_{I,j} = d_{I,j}(P'_{I-1,J} - P'_{I,J}) \end{cases} \quad \text{III.23}$$

Where : $d_{i,j} = \frac{A_{i,j}}{a_{i,j}}$ and $d_{I,j} = \frac{A_{I,j}}{a_{I,j}}$

NB : i,j : for staggered grid and I,J for scalar grid

We conclude that :

$$\begin{cases} u_{i,j} = u^*_{i,j} + d_{i,j}(P'_{I-1,J} - P'_{I,J}) \\ v_{I,j} = v^*_{I,j} + d_{I,j}(P'_{I-1,J} - P'_{I,J}) \end{cases} \quad \text{III.24}$$

Similar expression exist for $u_{i+1,J}$ and $v_{I,j+1}$:

$$\begin{cases} u_{i+1,J} = u^*_{i+1,J} + d_{i+1,J}(P'_{I,J} - P'_{I+1,J}) \\ v_{I,j+1} = v^*_{I,j+1} + d_{I,j+1}(P'_{I,J} - P'_{I+1,J}) \end{cases} \quad \text{III.25}$$

*The velocity fields should satisfy continuity equation:

$$[(uA)_{i+1,J} - (uA)_{i,J}] + [(vA)_{I,j+1} - (vA)_{I,j}] = 0 \quad \text{III.26}$$

$$\begin{aligned} & \left[A_{i+1,J} \left(u^*_{i+1,J} + d_{i+1,J}(P'_{I,J} - P'_{I+1,J}) \right) - A_{i,J} \left(u^*_{i,J} + d_{i,J}(P'_{I-1,J} - \right. \right. \\ & \left. \left. P'_{I,J}) \right) \right] - \left[A_{I,j+1} \left(v^*_{I,j+1} + d_{I,j+1}(P'_{I,J} - P'_{I+1,J}) \right) - A_{I,j} \left(v^*_{I,j} + \right. \right. \\ & \left. \left. d_{I,j}(P'_{I-1,J} - P'_{I,J}) \right) \right] = 0 \end{aligned} \quad \text{III.27}$$

This may be re-arranged to give:

$$\begin{aligned} [(dA)_{i+1,J} + (dA)_{i,J} + (dA)_{I,j+1} + (dA)_{I,j}]P'_{I,J} &= (dA)_{i+1,J}P'_{I+1,J} + (dA)_{i,J}P'_{I-1,J} + \\ (dA)_{I,j+1}P'_{I,J+1} + (dA)_{I,j}P'_{I,J-1} &+ [(u^*A)_{i,J} - (u^*A)_{i+1,J} + (v^*A)_{I,j} - (v^*A)_{I,j+1}] \end{aligned} \quad \text{III.28}$$

Identifying the coefficients of P' this may be written as :

$$a_{I,J}P'_{I,J} = a_{I+1,J}P'_{I+1,J} + a_{I-1,J}P'_{I-1,J} + a_{I,J+1}P'_{I,J+1} + a_{I,J-1}P'_{I,J-1} + b'_{I,J} \quad \text{III.29}$$

With :

$$a_{i+1,J} = (dA)_{i,J+1} ; a_{I-1,J} = (dA)_{I,j} ; a_{I,J+1} = (dA)_{I,j+1} ; a_{I,J-1} = (dA)_{I,j}$$

$$b'_{I,J} = [(u^*A)_{i,J} - (u^*A)_{i+1,J} + (v^*A)_{I,j} - (v^*A)_{I,j+1}] .$$

The previous equation represents the discretised continuity as an equation for pressure correction P'. The source term b' on the equation is the continuity imbalance arising from the incorrect velocity field u^*, v^* . By solving the equation, the pressure correction field P' can be obtained at all points. Once the pressure field is known, the correct pressure field may be obtained using the given formulas.

The omission of terms such as $\sum a_{nb}u'_{i,j}$ and $\sum a_{nb}v'_{I,j}$ in the derivation does not affect the final result because the pressure correction and velocity correction will all be zero in a converged solution giving $P^* = P; u^* = u; v^* = v$

The pressure correction equation is susceptible to divergence unless some under-relaxation is used during the iterative process and new, improved pressures P^{new} are obtained with $P^{new} = P^* + \alpha_P P'$ where α_P is the pressure under-relaxation factor.

Taking α_p between 0 and 1 allows us to add to guessed field P^* a fraction of the correction field P' that is large enough to move the iterative improvement process forward, but small enough to ensure stable computation.

The velocities are also under relaxed:

$$\begin{cases} u^{new} = \alpha_u u + (1 - \alpha_u)u^{(n-1)} \\ v^{new} = \alpha_v v + (1 - \alpha_v)v^{(n-1)} \end{cases} \quad \text{III.30}$$

u and v are velocities corrected without relaxation.

$u^{(n-1)}$ and $v^{(n-1)}$ velocities obtained in the previous iteration

So the momentum equations may take the form :

$$\begin{cases} \frac{a_{i,j}}{\alpha_u} u_{i,j} = \sum a_{nb} u_{nb} + (P_{I-1,J} - P_{I,J})A_{i,j} + b_{i,j} + \left[(1 - \alpha_u) \frac{a_{i,j}}{\alpha_u} \right] u_{i,j}^{(n-1)} \\ \frac{a_{l,j}}{\alpha_v} v_{l,j} = \sum a_{nb} v_{nb} + (P_{I-1,J} - P_{I,J})A_{l,j} + b_{l,j} + \left[(1 - \alpha_v) \frac{a_{l,j}}{\alpha_v} \right] v_{l,j}^{(n-1)} \end{cases} \quad \text{III.31}$$

The pressure correction is also affected velocity under-relaxation and it can be shown that the d terms of pressure correction equation become:

$$d_{i,j} = \frac{A_{i,j}\alpha_u}{a_{i,j}} ; d_{i+1,j} = \frac{A_{i+1,j}\alpha_u}{a_{i+1,j}} ; d_{l,j} = \frac{A_{l,j}\alpha_v}{a_{l,j}} ; d_{l,j+1} = \frac{A_{l,j+1}\alpha_v}{a_{l,j+1}}$$

Initial Guess P^*, U^*, V^*, ϕ^*

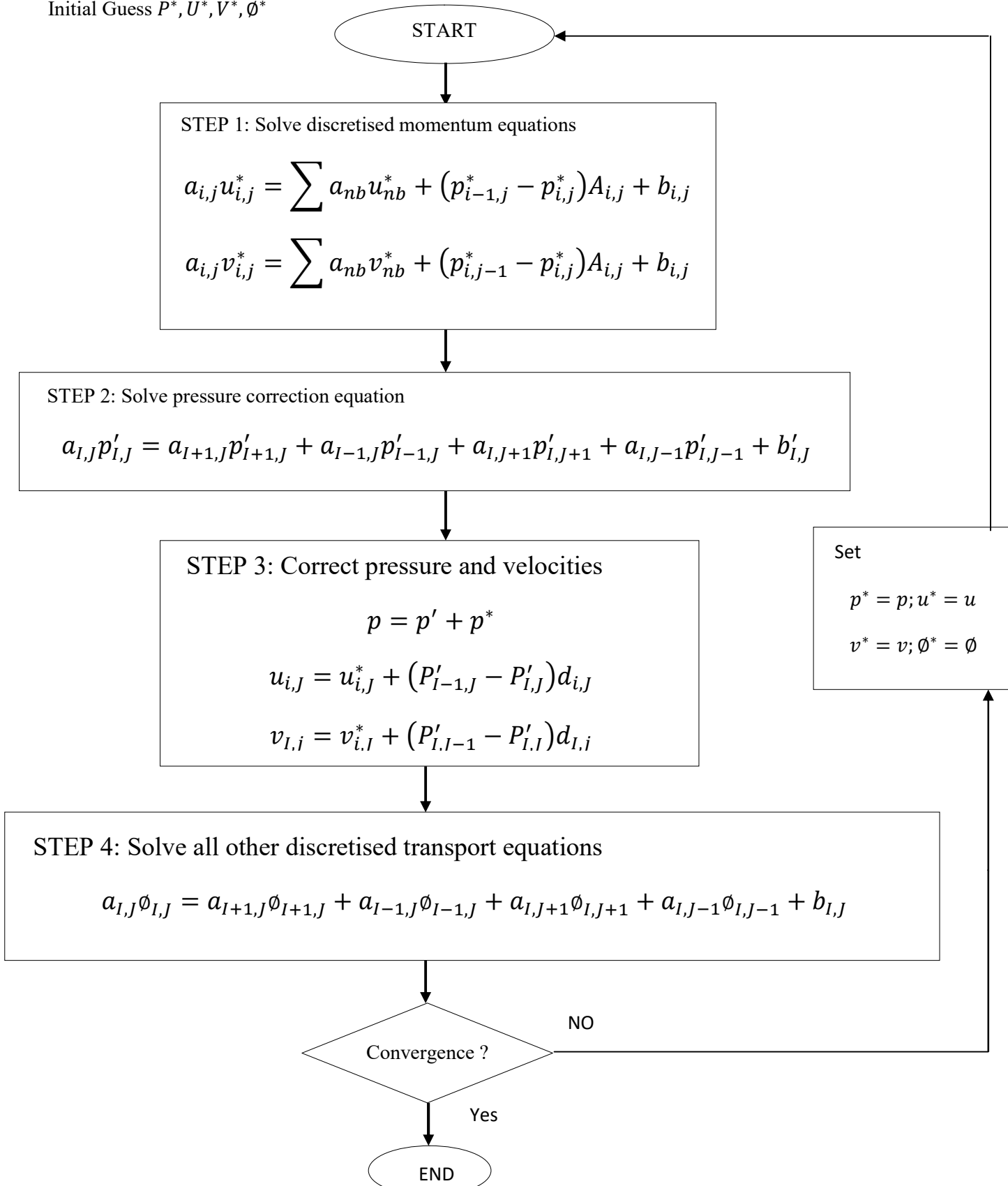


Figure III.3 : SIMPLE Algorithm

III.10-Conclusion :

In this chapter, we have presented th mathematical model for treating the problem and solve it using the SIMPLE algorithm. We gave a brief explanation about the discretisation of the physical domain and quantities and also the physical domain to simulate the system and get very accurate results shown on the next chapter.

CHAPTER IV :

RESULTS AND DISCUSSION

IV-1-Introduction:

In this chapter, we investigate steady state double diffusive mixed convection in a rectangular lid driven cavity under the combined buoyancy effects of thermal and mass diffusion. The heat and mass rates were examined using several operational dimensionless parameters, such as Richardson 'Ri', Lewis number 'Le', buoyancy ratio 'N' and Aspect ratio 'A'. The investigations were carried out for $0.1 \leq Le \leq 50$; $-10 \leq N \leq 10$; $0.01 \leq Ri \leq 10$ & $A = 0.5, 1, 2$. And the results were presented and highlighted in form of isocontours of velocities (streamlines), Temperature and Spices. The predicted results of both local and average Nusselt and Sherwood numbers are calculated and plotted.

IV-2-Algorithm validation:

The governing equation were solved by using finite volume method and following SIMPLE technique developed by Patankar [4], which is based on the discretisation of the governing equation.

In order to check the accuracy of the numerical technique employed for the solution of the problem imposed on the present work, The Algorithm validation was carried out in two folds. First, grid sensitivity tests were performed to inspect field variables grid-independency solution for the uniform node points of (20x20), (40x40), (60x60), (80x80), (100x100) were examined for the dimensionless parameters equal to unity : $Le=1, N=1, Ri=1$ ($Re=100$ & $Gr=10000$), $A=1, Pr=1$ and observing the variation of the average Nusselt number as shown on Figure 2, Adequate results can be achieved using the node points of (80x80) but we will use the node points of (100x100) for more accuracy and precision to ensure a high quality of results. In addition, To check the accuracy of the present numerical code we did a comparative study of isocontours of velocities, Temperature and concentration and also a local and average Nusselt & Sherwood Number of two works: **Al Amiri et al** [9] and **Teamah** [10].

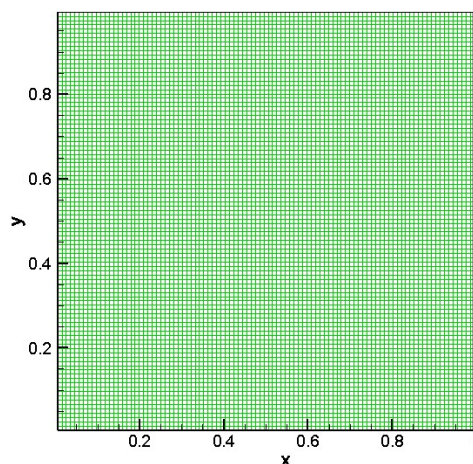
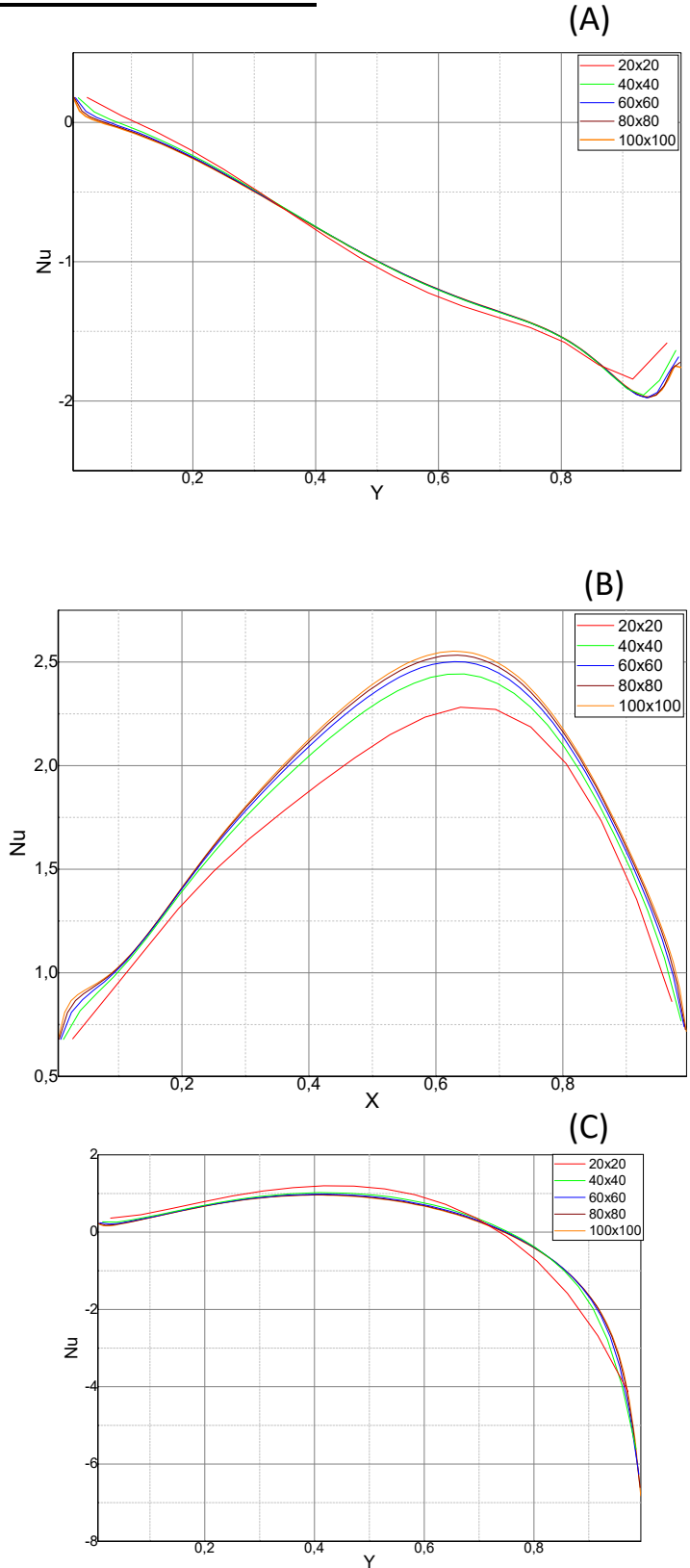


Figure IV.1: Used mesh

IV-2-1-The Local Nusselt number:



Figures IV.2: Variation of Nusselt Numbers along the different walls for different mesh grids

(A):Left wall; (B):Bottom wall; (C):Right wall

IV-2-2-The average nusselt number :

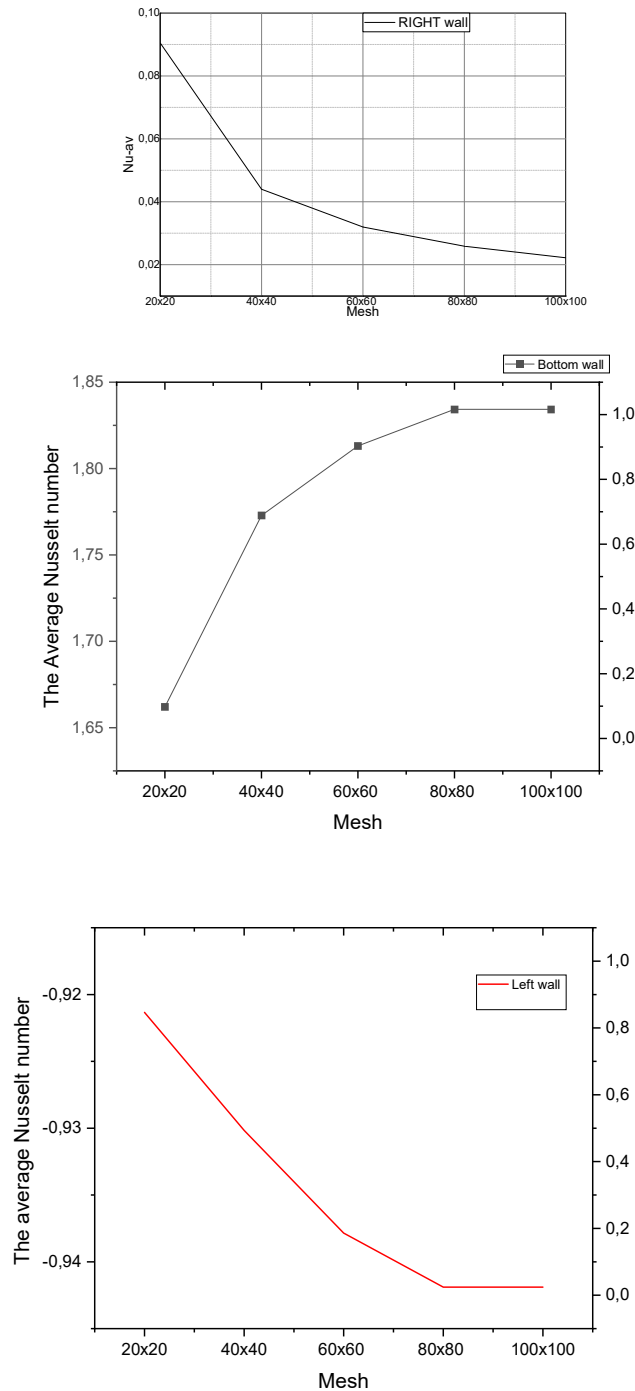


Figure IV.3: average Nusselt number at different walls for different grid mesh

The non dimensional governing equations were solved under the following relaxation factors, 0.5, 0.5, 0.7, 0.7 and 0.7 for u-velocity, v-velocity, Pressure, Temperature and concentration respectively. The residual must satisfy an error of 10^{-6} . And after observing the figures we realize that the grid of 100x100 is the best option for us to deal with the present problem.

IV-3-Comparative study with previous works:

In order to insure the accuracy of the computational method (SIMPLE) used for the present work. We compared our code results with two different published and validated results of articles on the lid-driven cavity flow of Al-Amiri *et al* and Teamh *et al*. The results are plotted using Tecplot 360 2008 version.

1-First validation: al-amiri *et al* [9]

The results shown below a comparaison of the streamfunction and isotherms and isoconcentration between AL-Amiri *et al* and the present work.

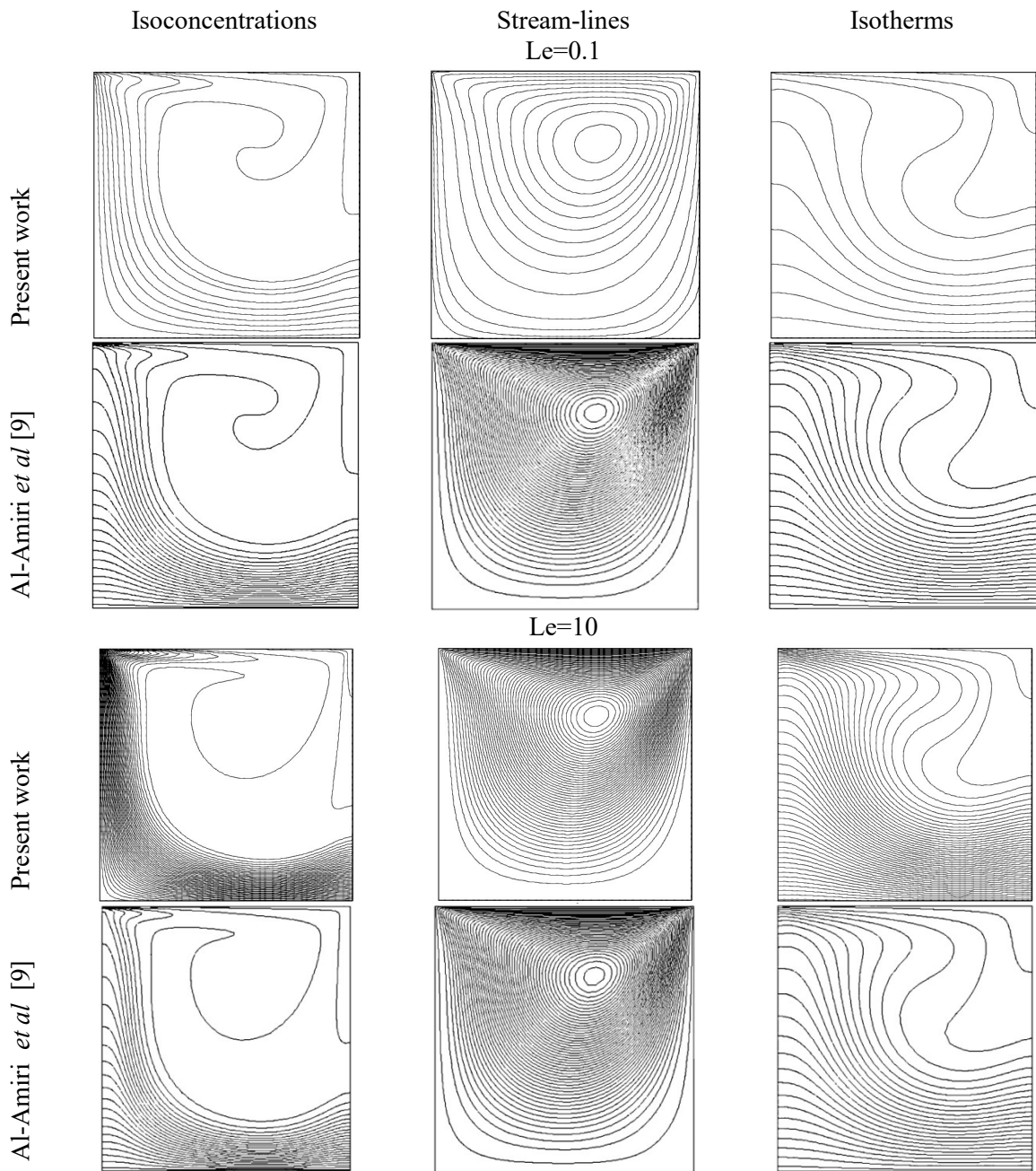


Figure IV.4: Isocontours of the present study and [9] for Le=0.1 Le=10

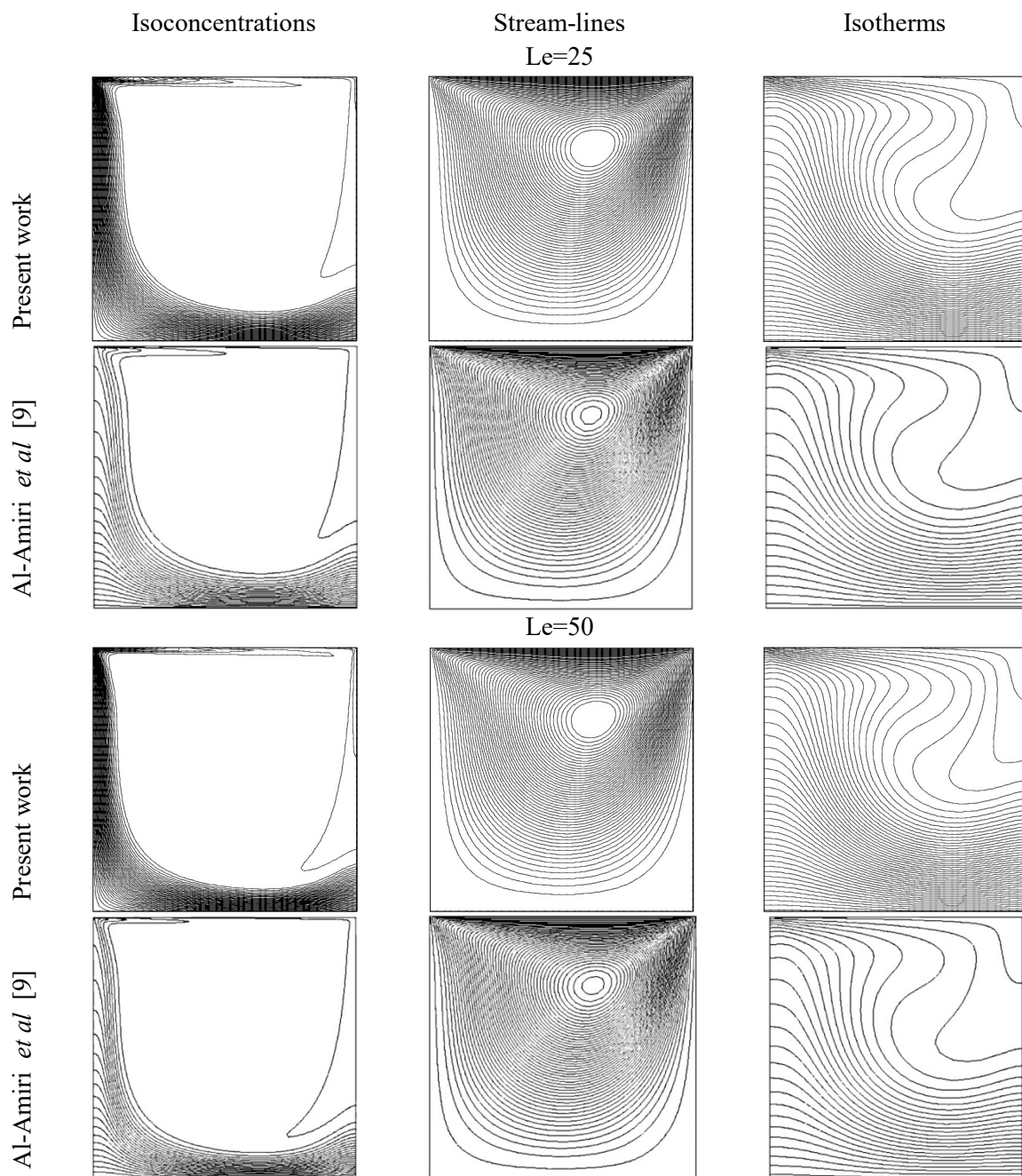


Figure IV.5: Isocontours of the present study and [9] for Le=25 and Le=50

The Results on the last figures shows that the there is an excellent agreement between our work and that of Al-Amiri *et al* which is another proof to validate the code and encourage us to manipulate the problem with it.

2-Second validation: Teamah et al [10]

The results shown below a comparison of the streamfunction and isotherms and isoconcentration between Teamah *et al* and the present work.

Comparative study of the effect of Lewis Number:

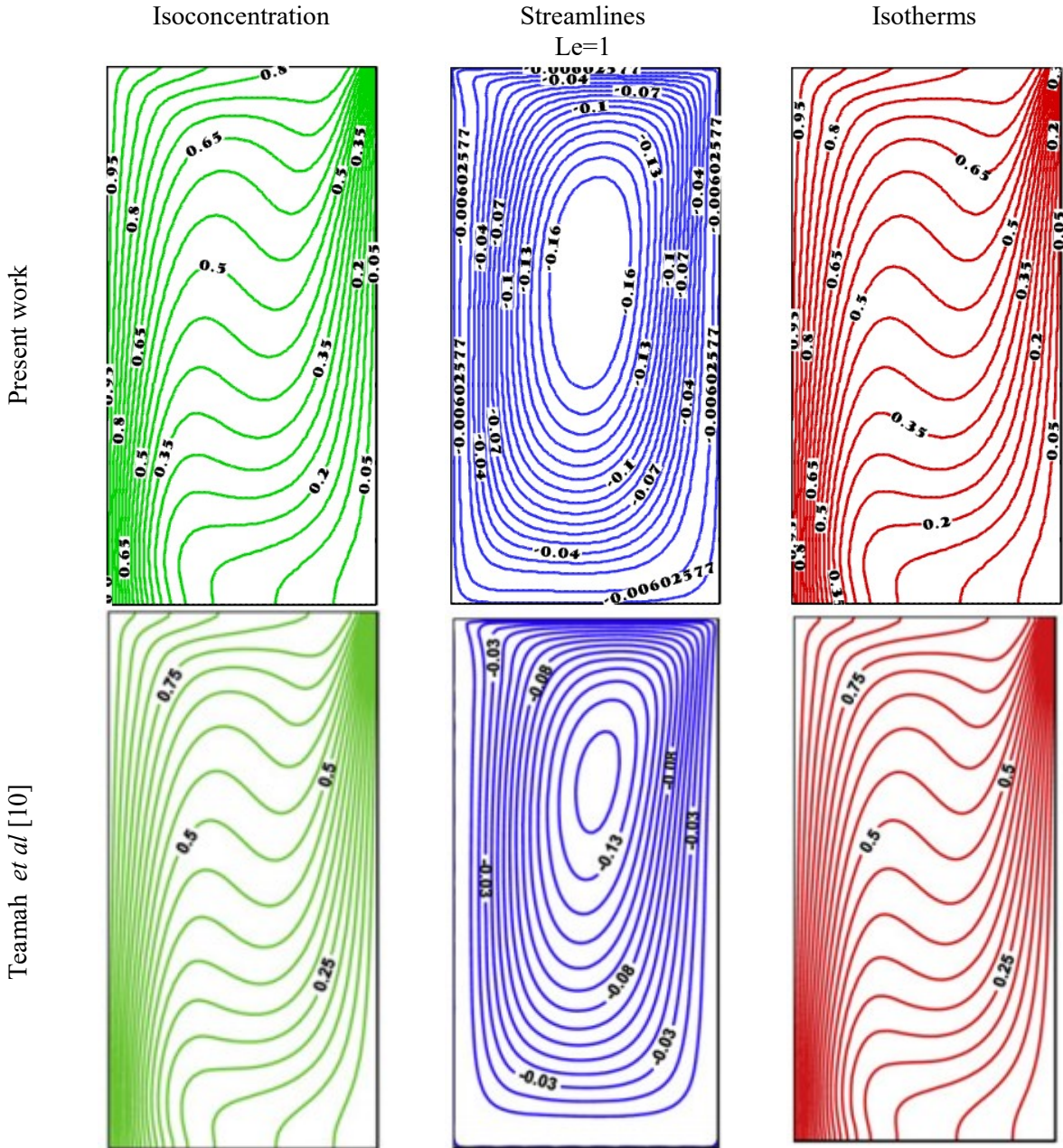


Figure IV.6: Isocontours of the present study and [10] for Le=1

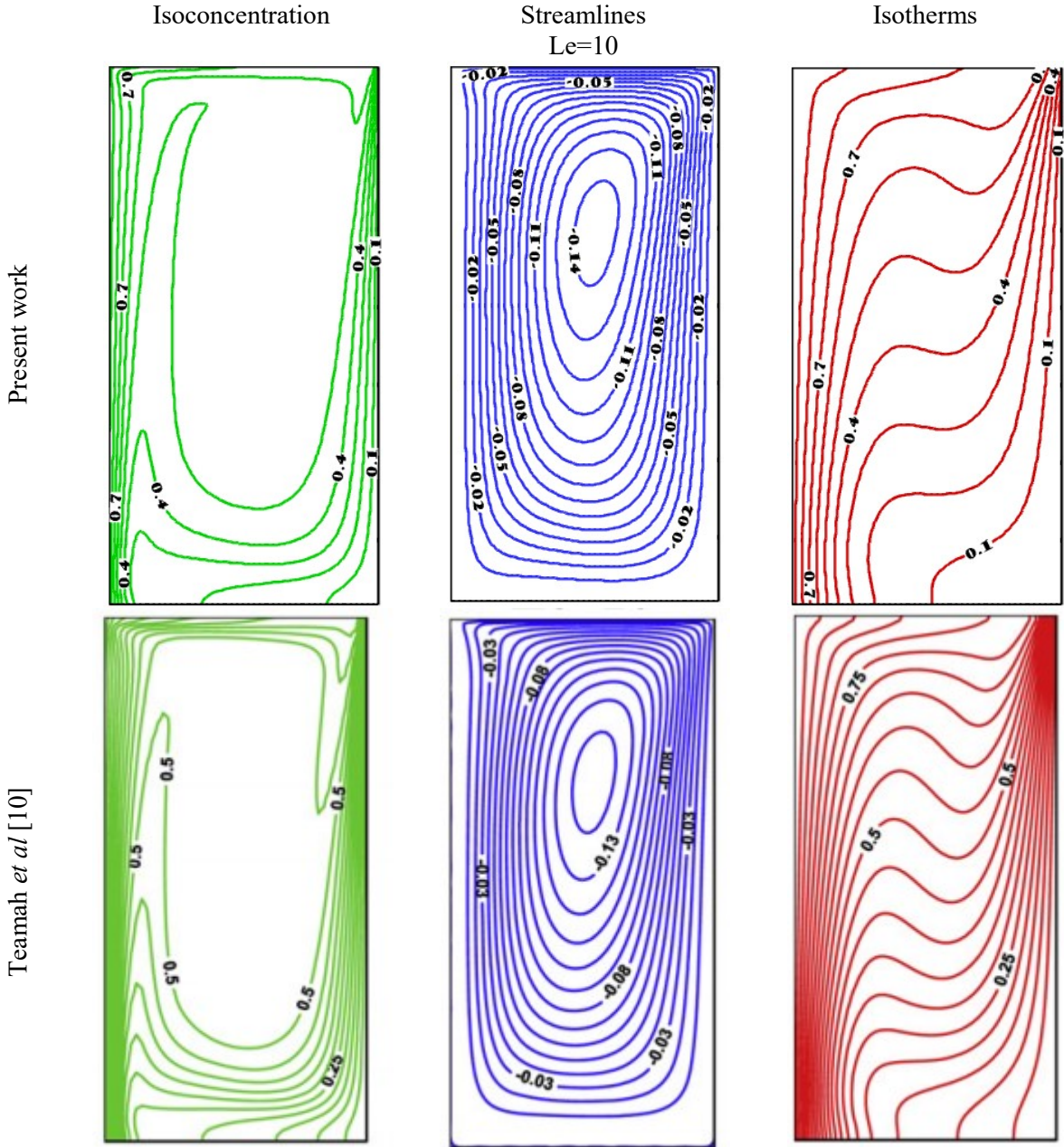


Figure IV.7: Isocontours of the present study and [10] for Le=10

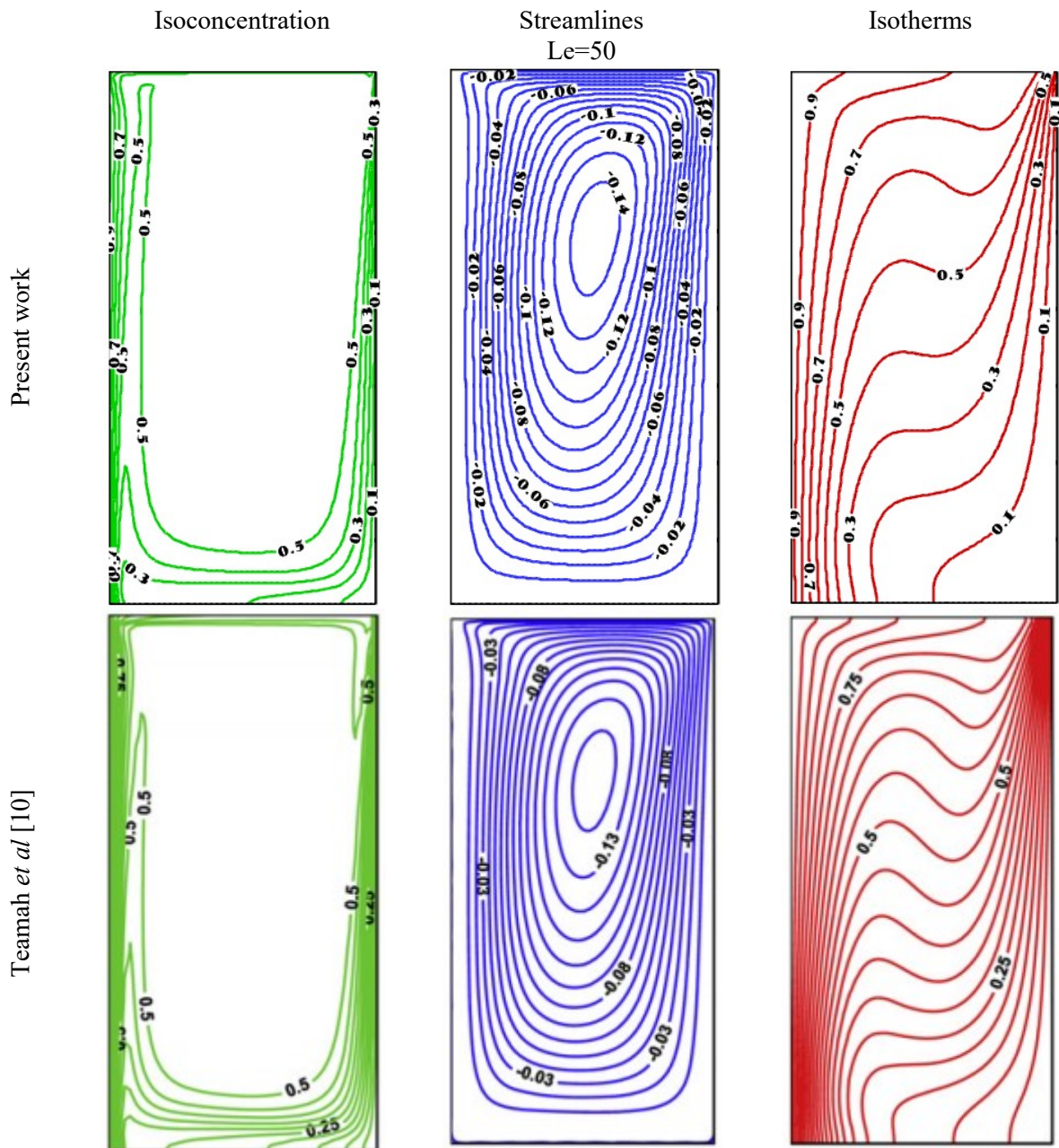


Figure IV.8: Isocontours of the present study and [10] for $Le=50$

Varying the Lewis number while $Pr=0.7$, $N=1$, $Ri=1$, $A=1$ like the Teamah *et al* did and we got perfect match of his results and ours.

For the second validation we have noticed a very good match with our work and Teamah *et al*'s work. So it's insuring to us that our code works very correctly and ready to be used for our problem.

3-An additional confirmation:

The graph below shows the different the average Nusselt number varying with Buoyancy factor of three works which are the present work , Teamah *et al* and Al-Amiri *et al* for the problem of al-Amiri *et al*. and the results show one more again a very good agreement of their codes and the numerical techniques which means they are all correct.

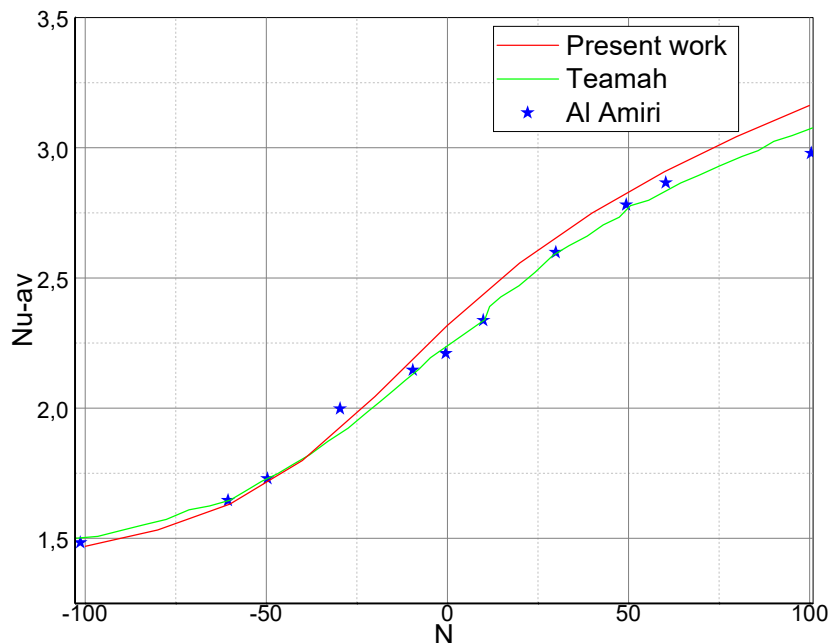


Figure IV.9: Average Nusselt number varying with N for present code and [9],[10] for the work of [9]

IV-4-Results and discussion :

On this section we will treat the main following variable for the present problem:

- The effect of Lewis Number which reflect the mass transfer on the rectangular enclosure.
- The effect of buoyancy ratio for both negative (opposing flow) and positive (assisting flow)
- The effect of Richardson number which characterize the importance of natural convection to forced convection.
- The effect of Aspect ratio which is the ratio between the height and the length of the studied cavity.
- Also the local and the average Nusselt and Sherwood numbers are presented.

IV-4-1-First case: effect of Lewis number Le

First of all, at the first look at the Figure IV.20 that shows the effect of Lewis number we can see clearly that this number has a direct effect to isoconcentration because every time we increase the value of Lewis number we observe a big change of the isocontours of the mass and the gradient of concentration increases the most at the left but basically there is an increase of the gradient at all the walls, which means an increase of mass transfer.

Second, we move to isotherms we saw a little bit of change at the isocontours of temperature there is a kind of stability of temperature gradient at the bottom wall. Generally there is a decreasing of heat transfer inside the cavity between $Le=0,1$ and $Le=1$ but there is not such a big difference in isotherms for $Le=1$ to $Le=50$.

There is no effect of Le at the isocontours of the velocity (Streamlines).

For the Local Nusselt number the Figure IV 21 shows a stability of Nusselt number at the left and right wall (specially for high Lewis number) which means there is not such a big difference between Nusselt numbers while varying with Lewis number, specially for high Lewis number ($Le>10$) but there is an obvious decreasing of Nusselt number for small value of Le number.

An important exchange of heat is situated at the top of side walls and at the middle of the bottom wall.

For the average Nusselt number the Figure IV 22 gives a general idea about heat transfer rates, and it seems constant with the variation of Lewis number (for high numbers Le).

NB: there is a decreasing of Nusselt number value from $Le=0,1$ to $Le=1$ which reflects to the decreasing of heat transfer rates.

For the Sherwood number (Local and average) the Figure IV 23 proves to us that there is an increasing of mass transfer (or increase of Sherwood number) rates with increase of Lewis number.

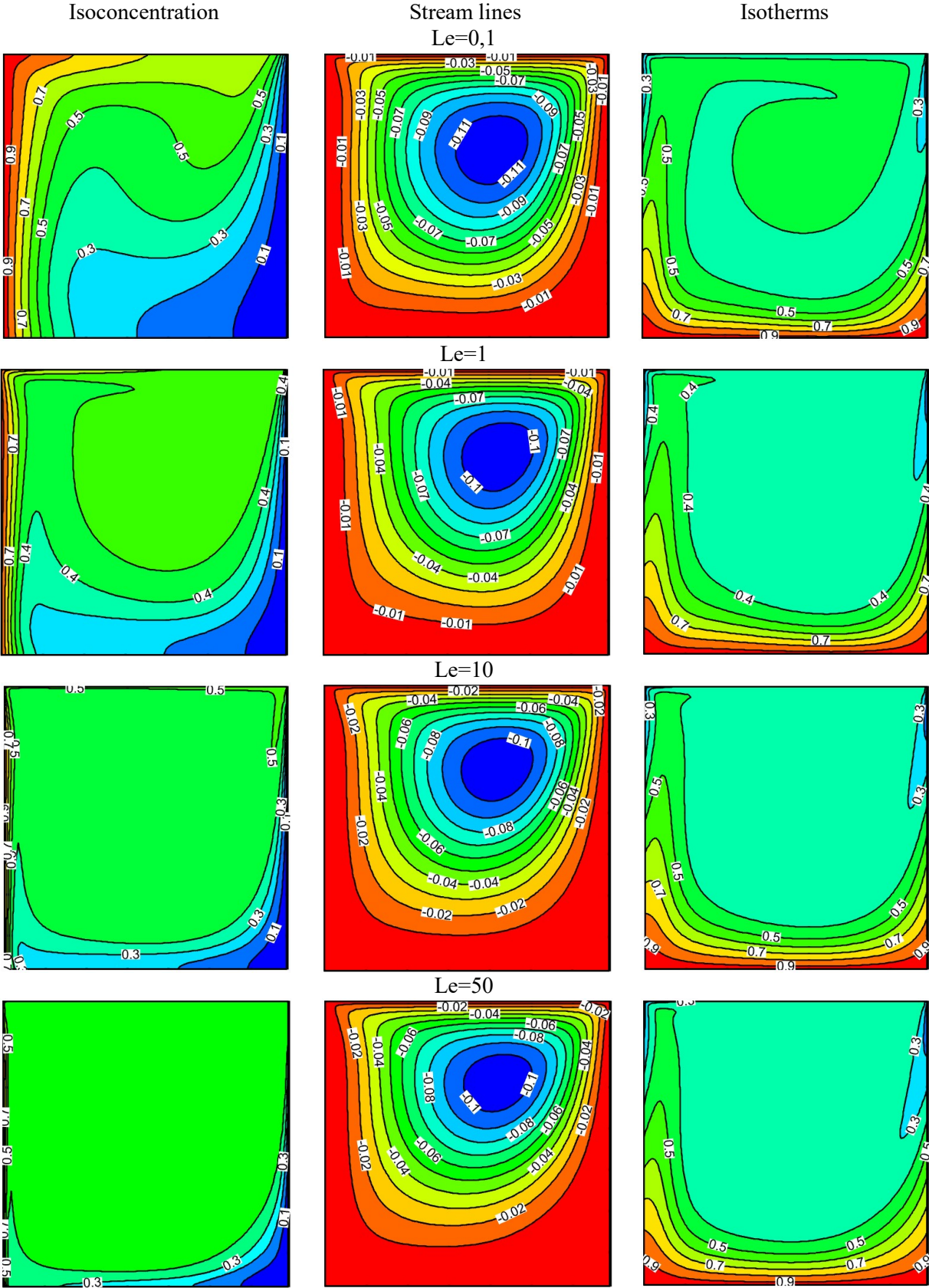
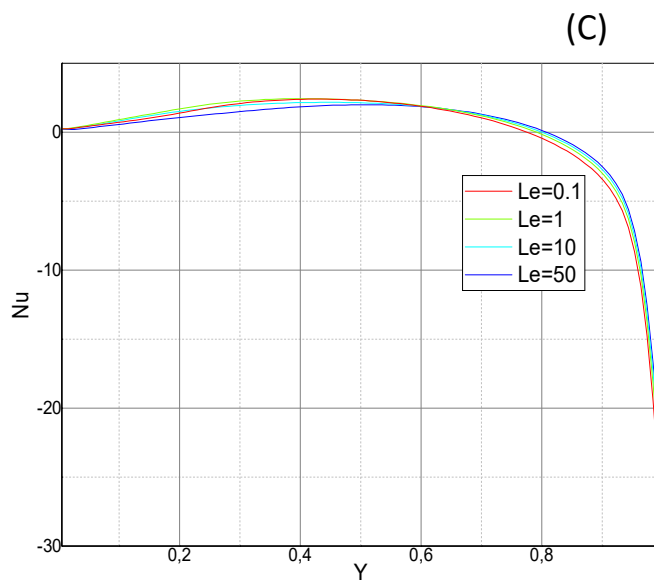
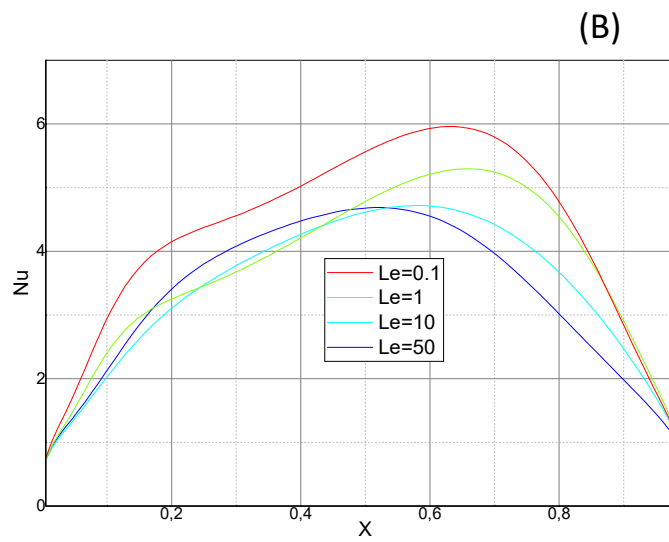
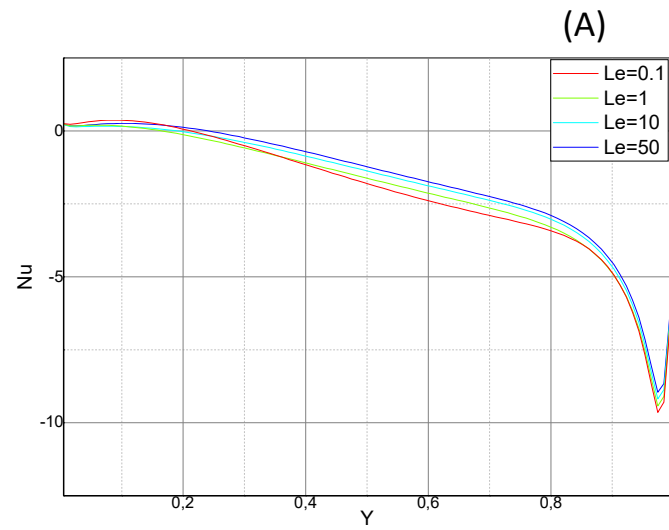


Figure IV.10: The effect of Lewis number on the isocontours for $N=1, Ri=1, A=1, Pr=10$



Figures IV.11: Nusselt number for Different walls $A=1, N=1, Ri=1$

(A):Left wall; (B):Bottom wall; (C):Right wall

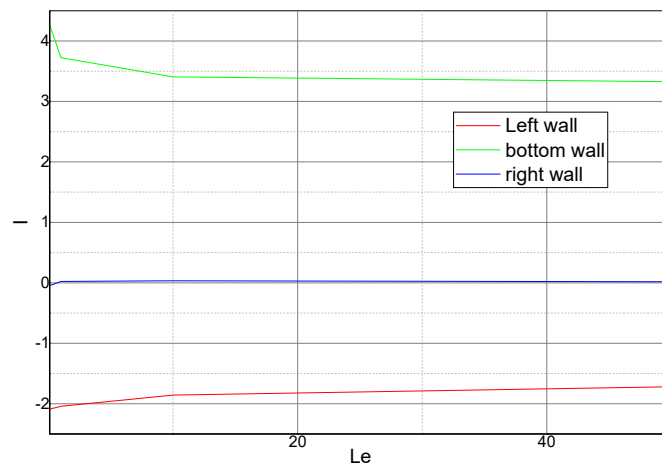


Figure IV.12: The average Nusselt number at the different walls varied with Le for $N=1, Ri=1, A=1$

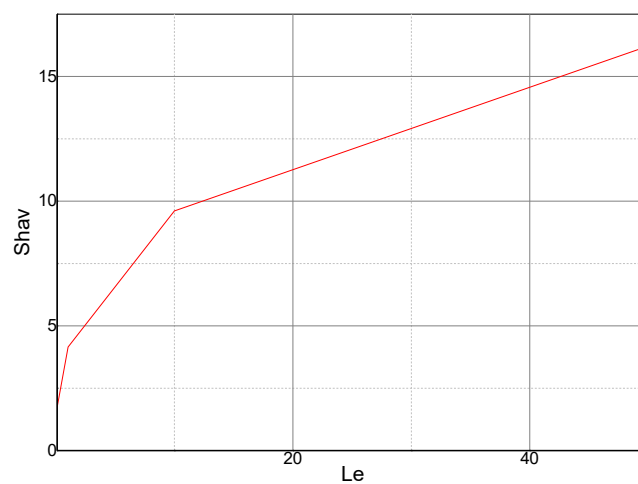
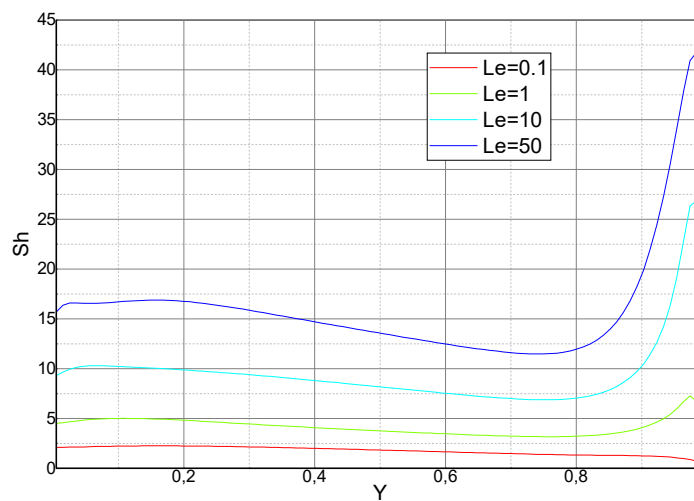


Figure IV.13: Local and average Sherwood number at the left wall varied with Le, $N=1, Ri=1, A=1$

IV-4-2-Second case: effect of buoyancy ratio N

After analyzing the Figure IV.24 that shows the effect of buoyancy ratio we can directly observe that this parameter has a direct effect on all isocontours.

Let's start with streamlines:

We can distinguish five different cases for five different values of N:

For $N=-10$ we got two big cells one caused by forced convection and the other caused by natural convection (and on it we saw q formation of two vortices inside this cell). And it is so clear that the buoyancy forces dominate forced convection.

For $N=-1$ we got also a formation of two big cells also like the previous one ($N=-10$) one caused by the lid-driven and the other caused by buoyancy forces and both of them have an effect to the fluid flow.

For $N=0$ it means the absence of the effect solutal buoyancy forces inside this cavity, so it's only under the effect of thermal buoyancy forces and forced flow. For this case ($N=0$) we got a formation of big cell (caused by forced convection) and another one smaller at right down corner of the cavity. it is so clear that the flow is dominated by forced flow.

For $N=1$ the buoyancy forces and forced flow flows in the same direction which result a one primary cell inside the cavity.

For $N=10$, it means that the intensity of mass buoyancy is much stronger (and after the equation II.8 we realize that the concentration term multiple by 10), and probably we can explain the change of the centre of the streamlines because the solutal buoyancy forces pushes the velocity vortices to the right wall.

For isotherms:

we saw a formation of cold area (cold vortices) for $N=-10$ and $N=-1$, also we can say the distribution of temperature increases with the increase of the absolute value of buoyancy ratio 'N' which refer an increasing of heat transfer rates.

For isoconcentration:

we observe an increase of the distribution mass all over the cavity with the increase of the absolute value of buoyancy ratio 'N', and also increase of the gradient of the concentration along the left wall with the increase of the absolute value of buoyancy ratio 'N' which refer an increasing of mass transfer rates.

For the Local and average Nusselt number we can't rely on the Figure IV.25 and Figure IV.26 because it didn't got such a direct information if the heat transfer rates increasing or decreasing.

NB: for this kind of problem I think probably the best option to see the effect of N on the Nusselt is to plot Nusselt number in absolute value.

But For the Sherwood number (Local And Average) the Figure IV.27 give us such a direct confirmation of our interpretation of the increase of mass transfer rates, because every time we increase the absolute value of buoyancy ratio we saw an increasing of Sherwood number and the average Sherwood number.

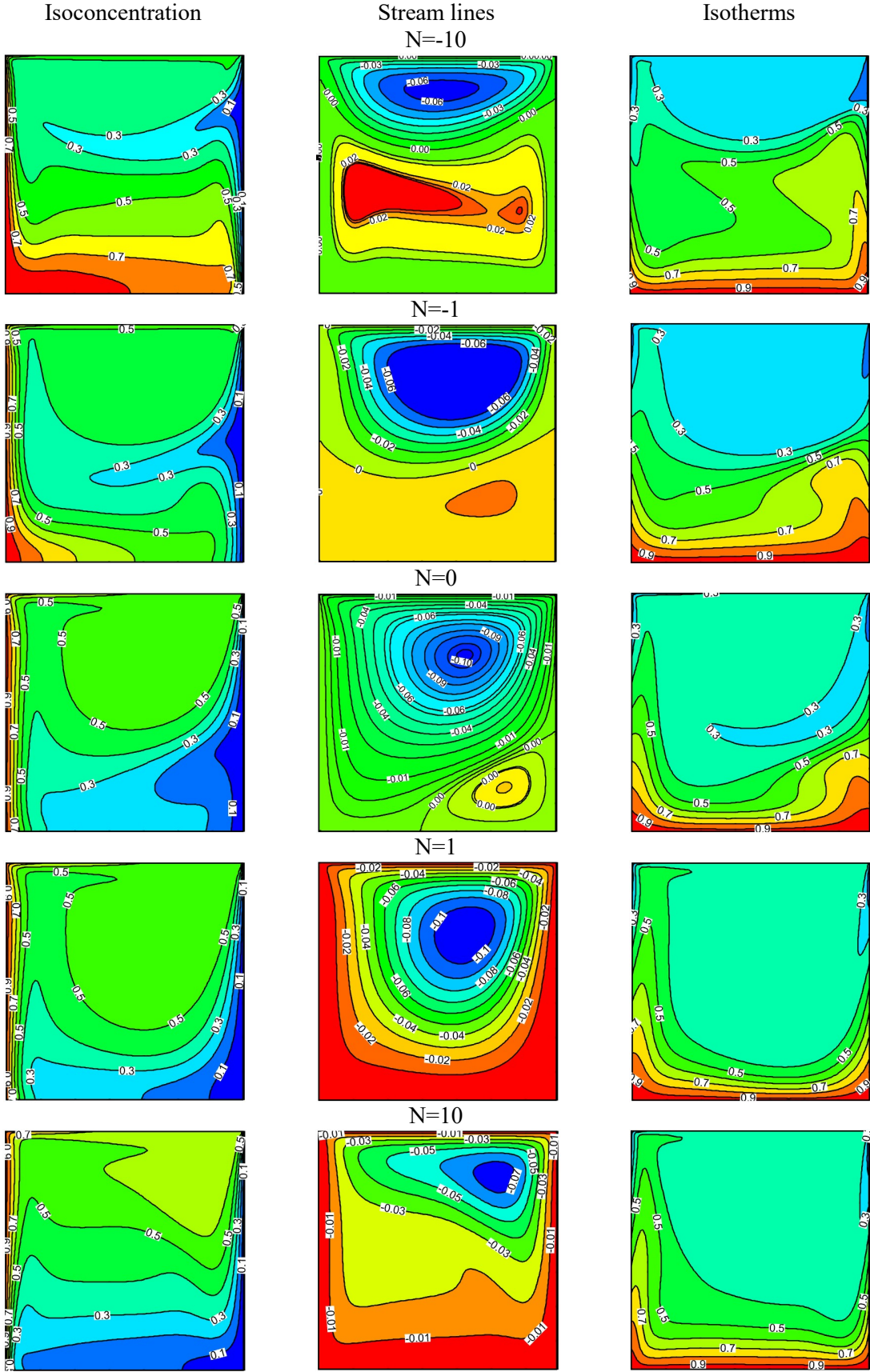


Figure IV.14: Effect of buoyancy ratio on the isocontours for $Le=1, Ri=1, A=1, Pr=10$

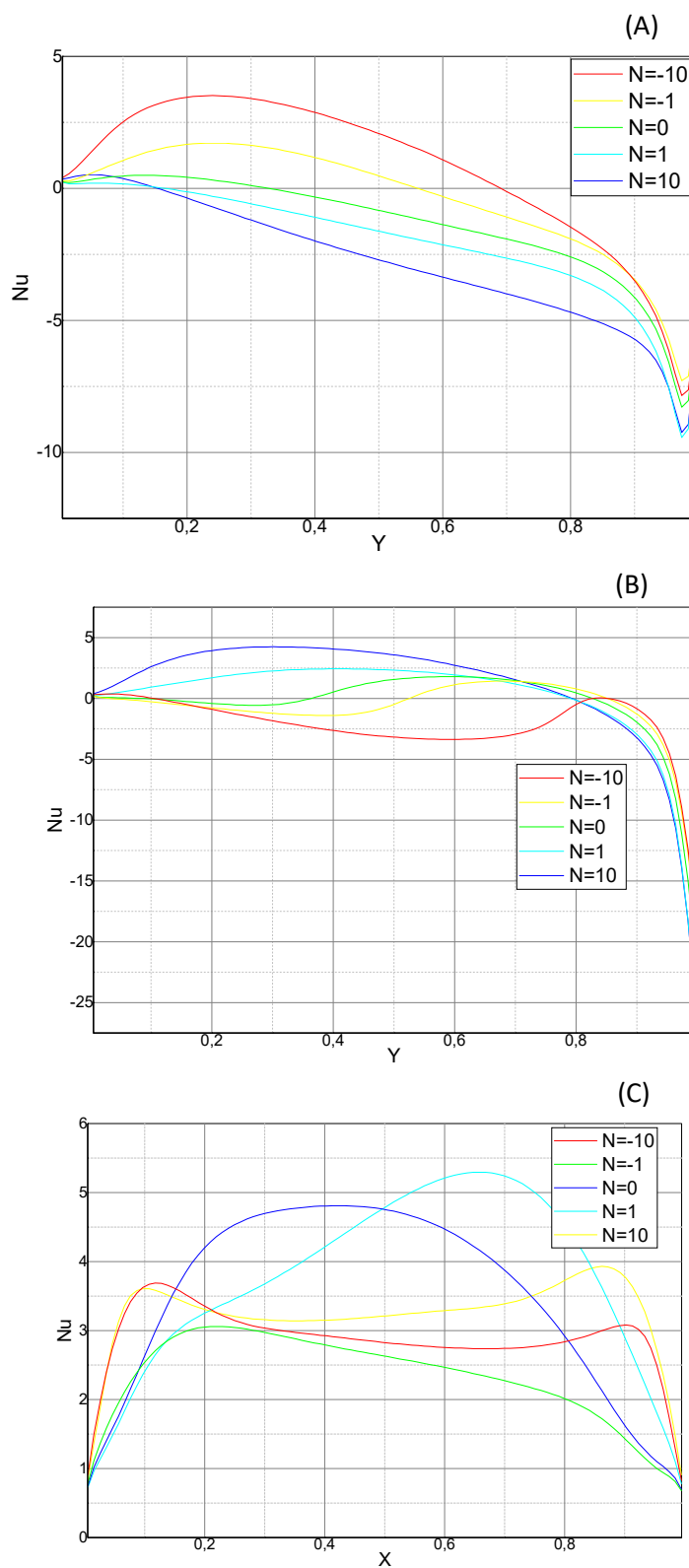


Figure IV.15: Nusselt number at the different walls varying with N while $Le=1, Ri=1, A=1$

(A) Left wall ; (B) Bottom wall ; (C) Right wall

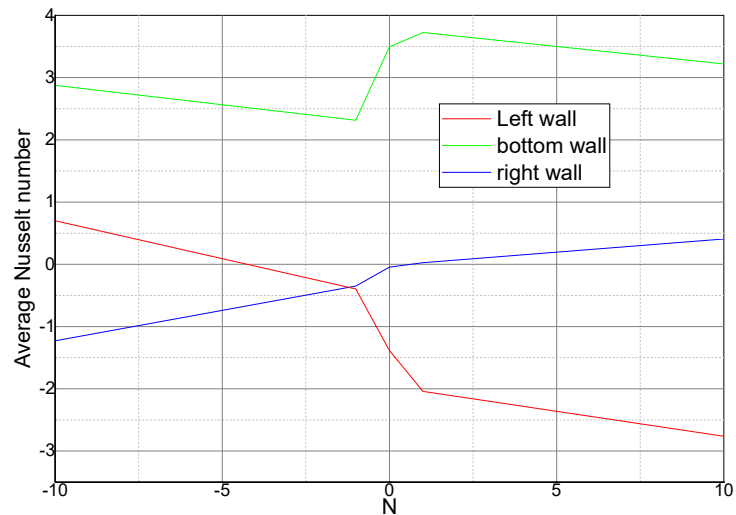


Figure IV.16: The average Nusselt number at the different wall varied with N $Le=1, Ri=1, A=1$

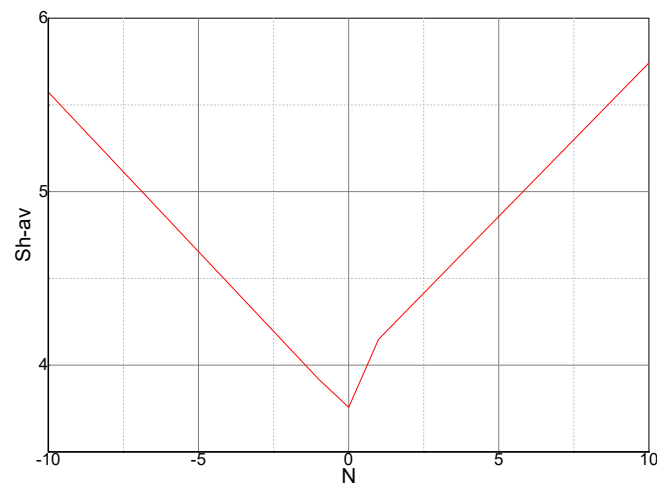
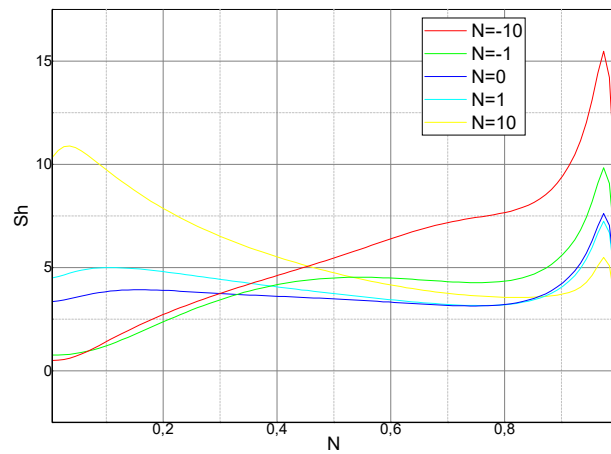


Figure IV.17: Local and average Sherwood number varied with N, while $Le=1, Ri=1, A=1$ at the left wall

IV-4-3-Third case: effect of Richardson number Ri :

The Figure IV.28 shown below proves to us that there is a significant effect of Ri number at all isocontours specially for high values of Ri number. The gradient of mass and temperature increases with the increase of Richardson number (with visual observation increase of these gradients in all the wall of the cavity).

Also for $Ri=10$ that means the intensity of mass and temperature is so high (according to the equation II.8 the solutal and thermal scalars multiple by 10)

For the Local Nusselt number, the Figure IV.29 show an increasing of this number with increase of Richardson number which refer an increasing of the heat transfer rates. Same thing can be concluded for average Nusselt number see Figure IV.30.

Also we observe at the Figure IV.31 an increasing of the Local Sherwood number and the Average Sherwood number with the increase of Richardson number which means an increase of mass transfer rates.

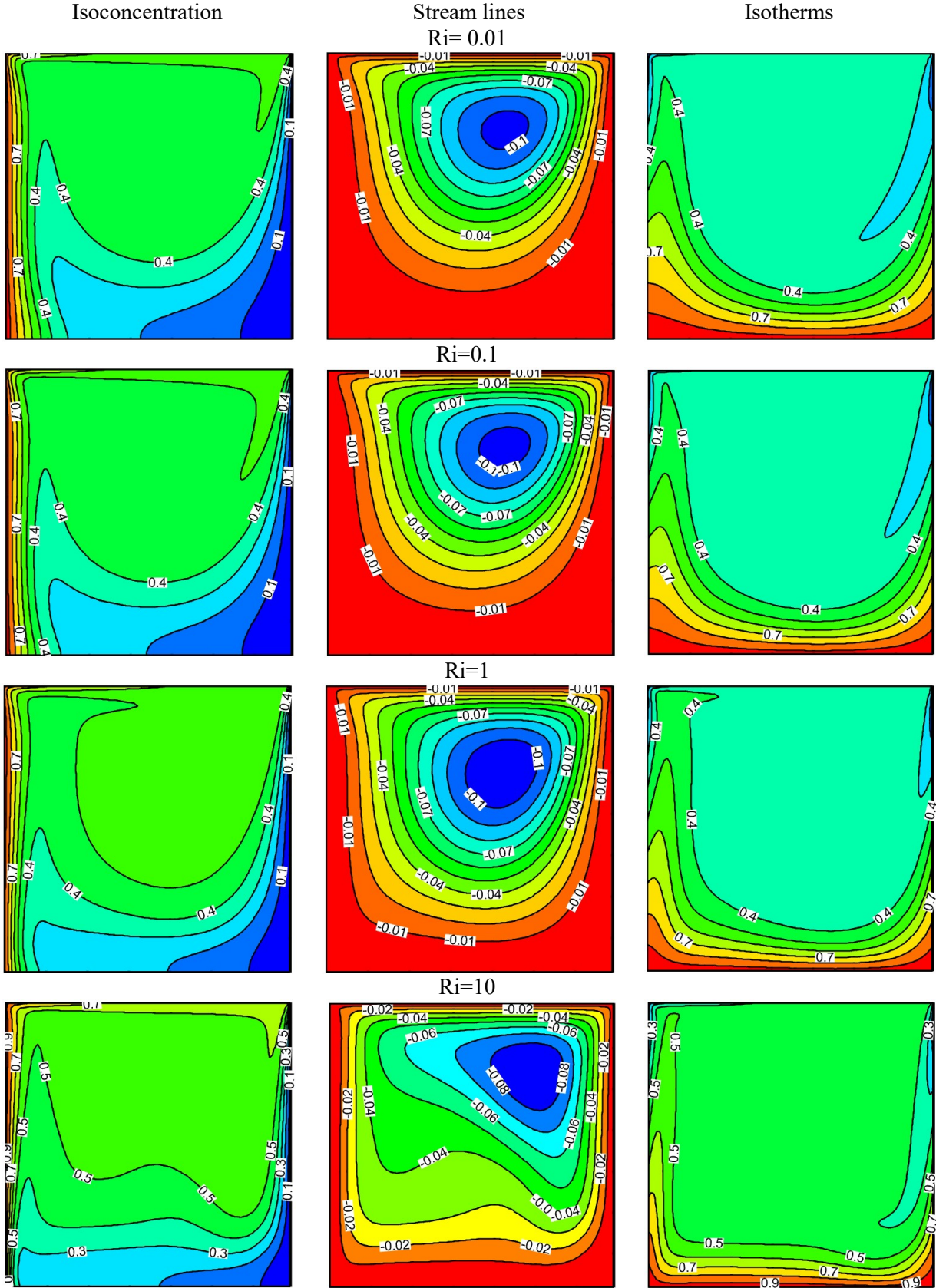


Figure IV.18: The effect of the Ri number on the isocontours while $Le=1, N=1, A=1, Pr=10$

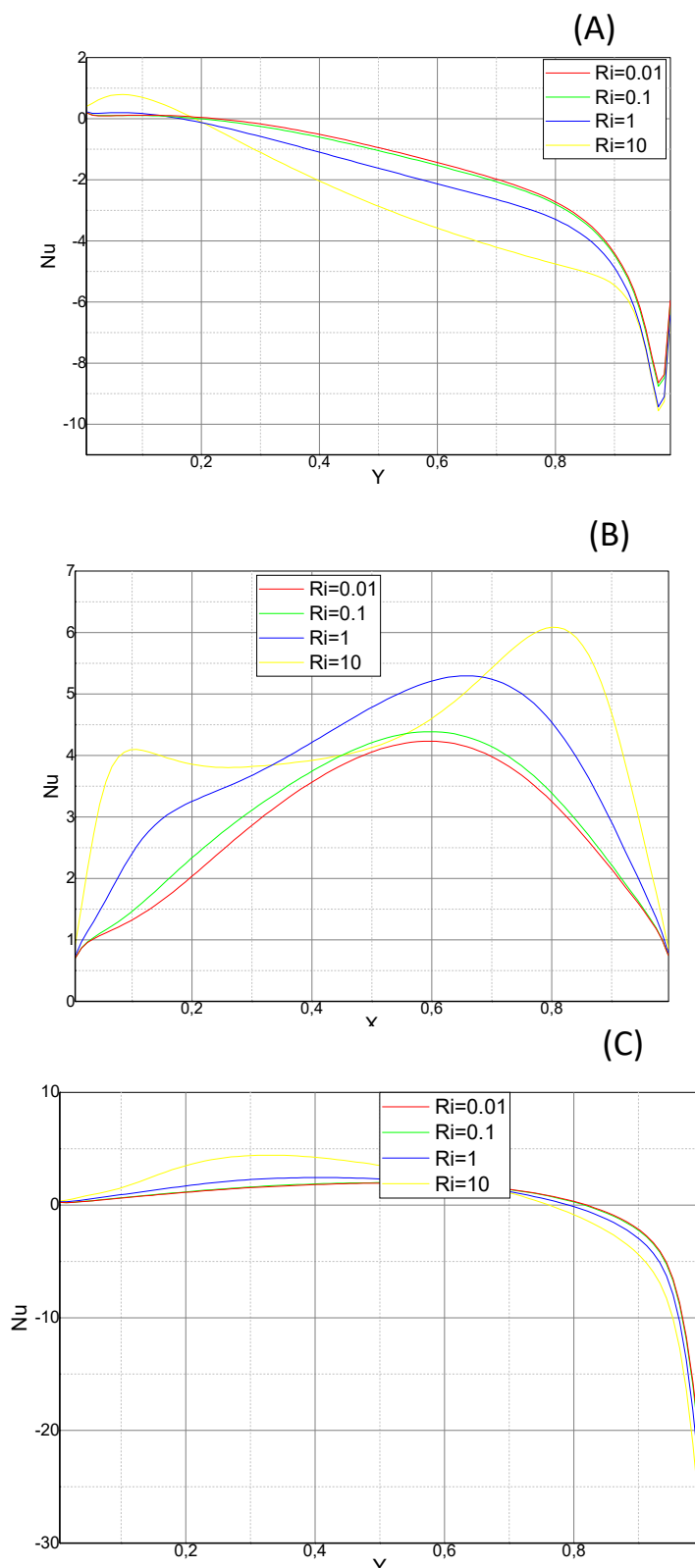


Figure IV.19: Nusselt number at the different walls for $Le=1, N=1, A=1$

(A):Left wall; (B):Bottom wall; (C):Right wall

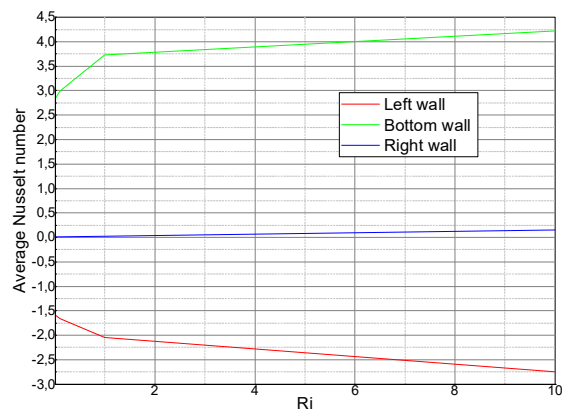


Figure IV.20: The average Nusselt number varied with Ri for different walls for $Le=1, N=1, A=1$

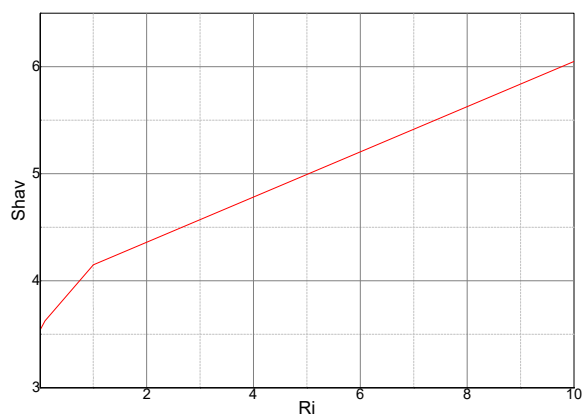
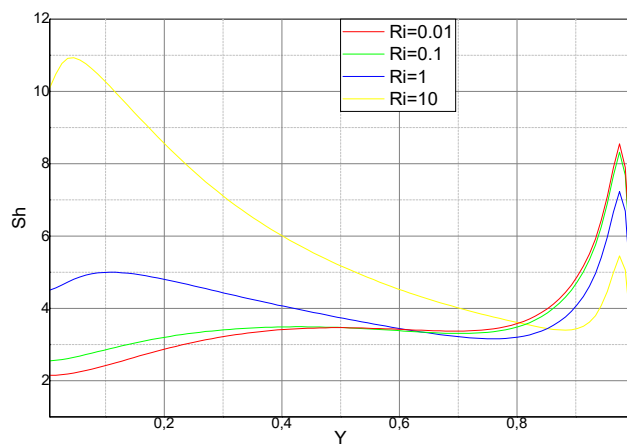


Figure IV.21: The local and average Sherwood number varied with Ri, for $Le=1, N=1, A=1$ at the left wall

IV-4-4-Fourth case: effect of Aspect ratio A:

After taking a general look at the figure we can say that:

For streamline:

We got unicell for $A=0,5$ and $A=1$ and a formation of two cells when $A=2$ because it gives buoyancy forces more space to interact well with the fluid flow.

For isotherms:

We saw a very good heating of the cavity when $A=0,5$.

Also an increase of heat transfers every time we increase of Aspect ratio.

Formation of two cells when $A=2$ for the presence of the effect of buoyancy ratio at this case $A=2$.

For isoconcentration:

The distribution of the mass is very usual there is no special effect of the Aspect ratio to the isoconcentrations except on the case when $A=2$ a formation of two cells.

Note: formation of two cells for all isocontours caused by significant presence of forced flow and buoyancy forces which appear in form of vortices.

For Local and average Nusselt number they are increasing with the increase of Aspect ratio 'A' hence to the augmentation of heat transfer area.

For local and average Nusselt number they are also increasing with increase of aspect ratio hence to the augmentation of mass transfer area.

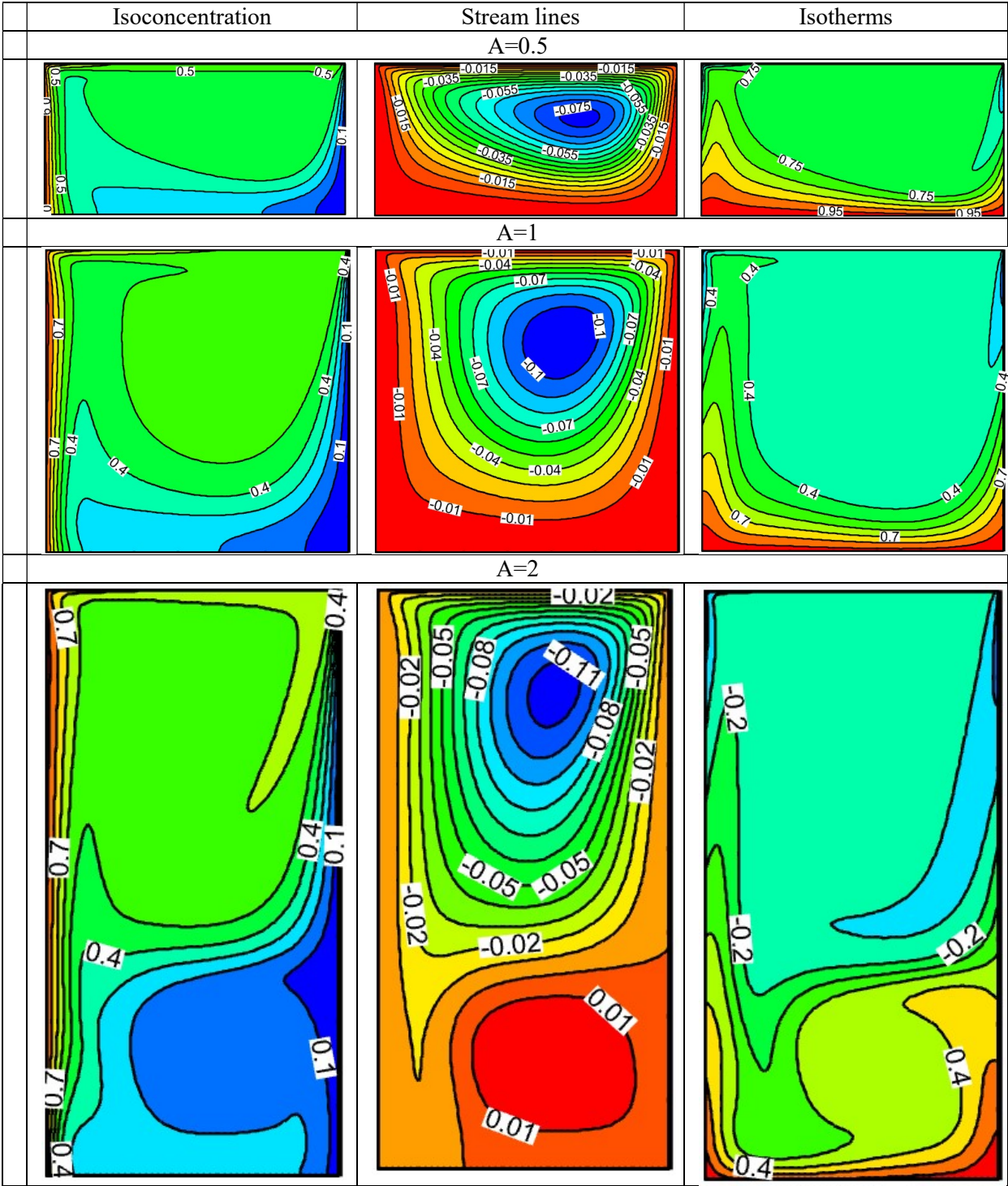


Figure IV.22: The effect of Aspect ratio on the isocontours while $Le=1, N=1, Ri=1$

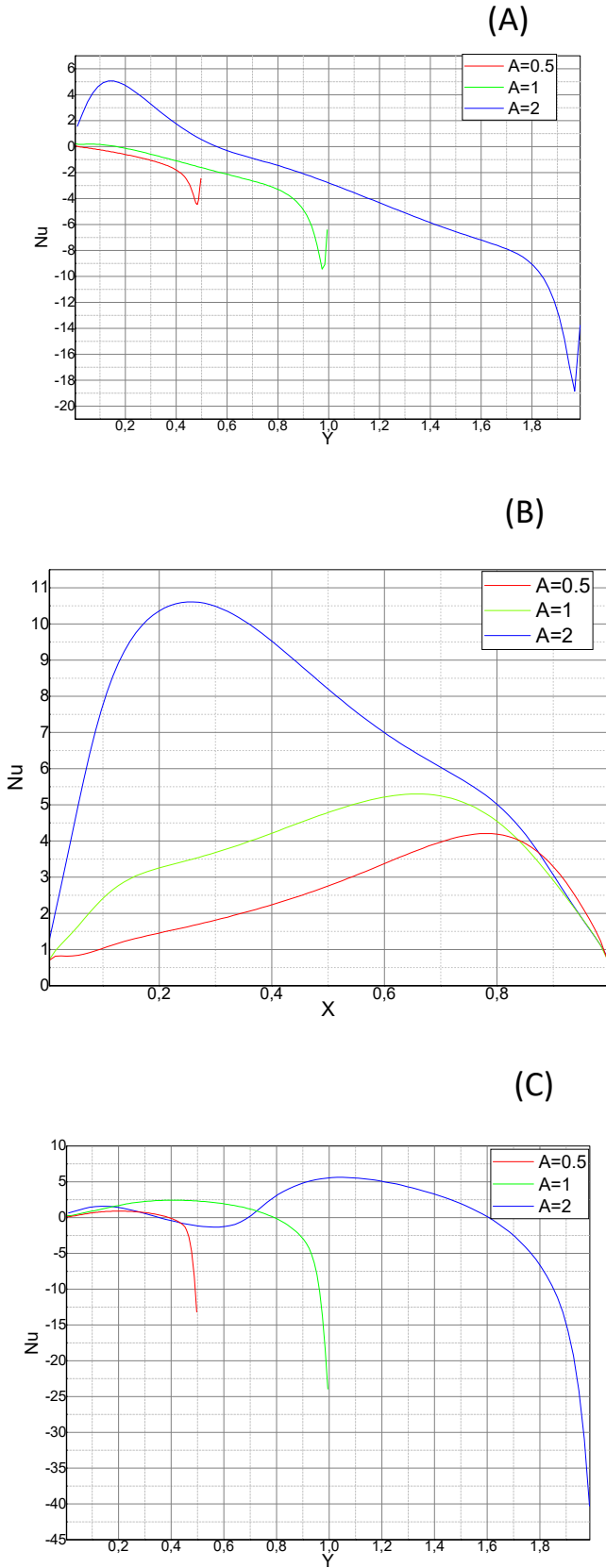


Figure IV.23: Nusselt number varied with Aspect ratio while Le=1, N=1, Ri=1

(A): Left wall; (B): Bottom wall; (C): Right wall

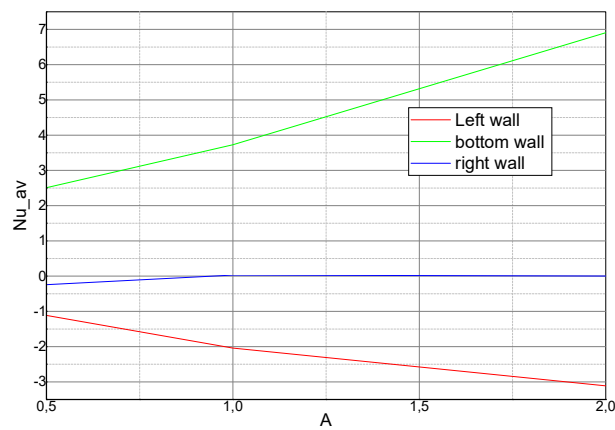


Figure IV.24: Average Nusselt number at different walls varied with Aspect ratio for $Le=1$, $N=1, Ri=1$

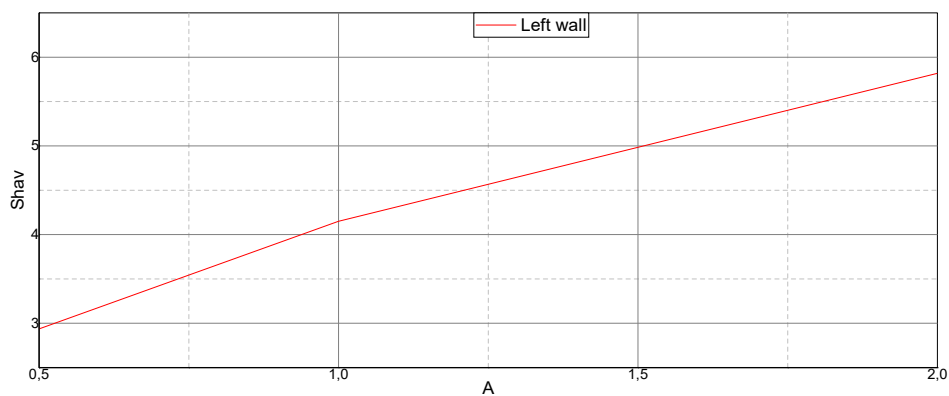
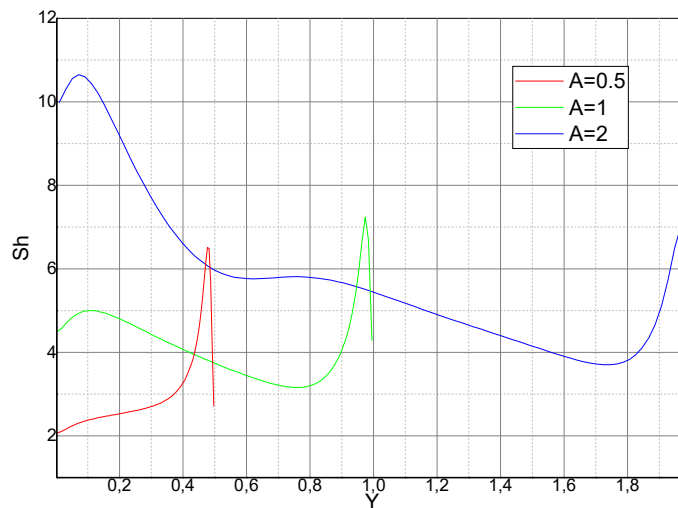


Figure IV.25: The local and average Sherwood number varied with Aspect ratio for $Le=1$, $N=1, Ri=1$ at the left wall

IV-5-Conclusion:

In this chapter, we have presented a comparative study of the isocontours of velocities, temperature and concentration between our code results and two other published works which means that's work very correctly then we treated the current work which varying the dimensionless parameters Le, N, Ri, A for fixed $Pr=10, Re=100$ then we plotted the different isocontours and the different Nusselt and Sherwood number along the different walls.

V- GENERAL CONCLUSION

GENERAL CONCLUSION:

The work presented in this thesis is a numerical study of heat and mass transfer of an incompressible fluid flow inside a rectangular cavity with a movable upper wall moves to the right. The mathematical modeling of this physical problem is based on the conservation equations of mass, momentum, energy and species. The thermo-physical properties are considered constant and the Boussinesq approximation has been adopted. Simplifying assumptions have been introduced and justified. The simplified system of equations is solved numerically by the finite volumes method. The velocity-pressure coupling is processed by the SIMPLE algorithm.

A computer code was developed and validated in comparison with the numerical results available in the literature.

The main results from this work can be summarized as follows:

- The rate of heat and mass transfer increase with increasing of Richardson number
- The variation of the Lewis number has no significant effect on the heat transfer except for small values of Lewis there is a decreasing of heat transfer rates but it needs a detailed study to confirm this hypothesis; on the other hand, an increase in the value of the Lewis number favors the mass transfer.
- Heat and mass transfer rates increase with increasing buoyancy ratio N (in absolute value).
- increase in aspect ratio implies an increase in heat and mass exchange surface therefore an increase in mass and heat transfer.

References:

- [1] W. M. Kays, M. E. Crawford, convective Heat and Mass Transfer, 3rd Edition ,McGrawHill,1993
- [2] A. S. Lavine, F. P. Incropera, D. P. DeWitt, Fundamentals of Heat and Mass Transfer ,eighth Edition, WILEY,2017
- [3] J.Lienhard IV and J..Lienhard V,A Heat and Mass transfer Textbook, 3rd Edition, J..Lienhard V,2001
- [4] S.V.Patankar, Numerical Heat Transfer and Fluid Flow, McGrawHill, 1983
- [5] H.K.V.W Malalasekera , An Introduction to Computational Fluid Dynamics The Finite Volume Method, Longman Group,1995
- [6] Online code learning under the BYJU'S Group ,07/01/2022,<https://byjus.com/>
- [7] Non-profit project, built entirely by a group of young engineers. The entire website is based on their personal perspectives, 07/01/2022,www.nuclear-power.com
- [8] Thermal engineering is a specialized discipline of mechanical engineering that deals with the movement of heat energy and transfer. 07/01/2022,<https://www.thermal-engineering.org/>
- [9] A. M. Al-Amiri, K. M. Khanfer, Ioan Pop, Numerical simulation of combined thermal and mass transport in a square lid-driven cavity, International Journal of Thermal Sciences, 46 (2006), 662-671.
- [10] M. A. Teamah, W. M. El-Maghlany, Numerical simulation of double-diffusive mixed convective flow in rectangular enclosure with insulated moving lid, International Journal of Thermal Sciences, 49 (2010),1625-1638.
- [11] B. Mefteh, A. Hassan , Natural convection in an inclined rectangular enclosure filled by CuO–H₂O nanofluid, with sinusoidal temperature distribution, International Journal of Hydrogen Energy vol. 40 (2015). 39, Pages: 13676--13684, DOI: 10.1016/j.ijhydene.2015.04.090
- [12] M. Sathiyamoorthy, T.Basak; S. Roy, I. Pop (2007) Steady natural convection flows in a square cavity with linearly heated side wall(s),International Journal of Heat and Mass Transfer vol. 50 iss. 3-4,Pages: 766--775, DOI: 10.1016/j.ijheatmasstransfer.2006.06.019

[13] Y. Stiriba, Analysis of the flow and heat transfer characteristics for assisting incompressible laminar flow past an open cavity, *International Communications in Heat and Mass Transfer* vol. 35 iss. 8 2008, Pages: 901-- 907, DOI: 10.1016/j.icheatmasstransfer.2008.04.004

[14] Simulation software website , What is Transport Equation ,07/01/2022, <https://www.simscale.com/docs/simwiki/numerics-background/what-is-the-transport-equation/>